(Miltenyi Biotec, Bergisch Gladbach, Germany, http://www.miltenyibiotec.com). After purification, over 95% of the separated cells were confirmed to be $CD34^+$ by flow cytometric analysis (data not shown). Each experiment was performed with cord blood $CD34^+$ cells derived from the same sample.

Suspension Cultures

Purified $CD34^+$ cells were seeded at a cell density of $1–2 \times 10^4$ cells per milliliter in 24-well tissue plates (Falcon, Becton, Dickinson and Company, Franklin Lakes, NJ, http://www.bd.com) with QBSF-60 serum-free medium (Quality Biological, Inc., Gaithersburg, MD, http://www.qualitybiological.com) containing SCF (100 ng/ml), FL (100 ng/ml), TPO (10 ng/ml), IL-6 (100 ng/ml), and sIL-6R (100 ng/ml). Cells were cultured in humidified air with 5% CO_2 at 37°C.

Protein Delivery

Synthetic peptides were delivered into 293T and CB $CD34^+$ cells using the Profect Protein Delivery System (Targeting Systems, Santee, CA, http://www.targetingsystems.com) according to the manufacturer's instructions.

Colony Assays

Cells were seeded into methylcellulose medium (MethoCult GF H4434V; Stem Cell Technologies, Vancouver, BC, Canada, http://www.stemcell.com) at a density of 2.5×10^2 cells per 35-mm dish and were cultured with 5% CO_2 at 37°C. All cultures were performed in triplicate, and the numbers of colonies were counted after 10 days.

Reconstitution Assays Using NOD/SCID Mice

Transplantation assays using NOD/SCID mice were performed according to procedures described previously [4] with some modifications. Briefly, 6–8-week-old NOD/SCID mice were total-body irradiated (TBI) with a dose of 2.4 Gy (60 Co) and then transplanted with the whole of peptide-treated cells or 2×10^4 freshly isolated $CD34^+$ cells through the tail vein. Because natural killer cell activity is retained in NOD/Shi-scid mice, the recipients were injected i.p. with 400 μl of phosphate-buffered saline containing 20 μl of anti-asialo-GM1 Ab immediately before cell transplantation. Identical treatments were performed on days 7 and 14. The proportion of reconstituted human cells in peripheral blood (PB) or bone marrow (BM) was assessed by flow cytometry with the anti-human CD45 Ab. For secondary transplantations, bone marrow cells were obtained from tibiae and femurs of the first mice that received transplants 12 weeks after transplantation, and 0.5×10^7 total bone marrow chimeric cells were injected into secondary NOD/SCID recipients subjected to immunosuppressive treatment before and after transplantation as described above ($n = 5$). Six weeks after transplantation, the presence of transplanted human cells in recipient BM was confirmed by flow cytometry as described above.

Limiting Dilution Analysis

The frequencies of human HSCs that were capable of repopulating in NOD/SCID mice in freshly isolated CB $CD34^+$ cells and peptide-treated cells were quantified by a limiting dilution analysis as described previously [46–48]. In this analysis, to avoid graft rejection, the recipients were treated with TBI in combination with anti-asialo-GM1 Ab immediately before and after transplantation (days 7, 14, 21, and 28). Data from several limiting dilution experiments were pooled and analyzed by applying Poisson statistics to the single-hit model. Frequencies were calculated using the maximum likelihood estimator.

Luciferase Assays

The details of the −1,137-c-*myc*-Luc vector, containing a 1,653-base pair (bp) fragment of the c-*myc* promoter (–1,137 to +516), were described previously [49]. To construct 3 × HB4(–316)-Luc and 3 × HB4(–72)-Luc, three tandem repeats of HOXB4-responsive elements at the indicated positions in the insulin-like growth factor-binding protein (IGFBP)-1 promoter were subcloned into pGL3 basic-TK-Luc. The sequences of the HOXB4-responsive elements were as follows: HB4(–316), 5′-CTTGTGTCAATTAAAGA and HB4(–72), 5′-GCGCTGCCCAATCATTAA. Luciferase assays were performed with a Dual-Luciferase Reporter System (Promega, Madison, WI, http://www.promega.com) as previously described [50]. Briefly, 293T cells (2×10^5 cells) were seeded in a 60-mm dish and cultured for 24 hours. Using the calcium phosphate coprecipitation method, cells were transfected with 6 μg of pcDNA3-HOXB4 alone or in combination with 6 μg of pCS2-PBX1a, along with 2 μg of reporter gene and 10 ng of pRL-CMV, a *Renilla* luciferase expression vector. After 12 hours, cells were washed, serum-starved for 24 hours, and subjected to luciferase assays. In some experiments, various doses of synthetic peptides were delivered into 293T cells 24 hours prior to luciferase assays.

Electrophoretic Mobility Shift Assay

Electrophoretic mobility shift assay (EMSA) was performed as previously described [51]. The double-stranded oligonucleotide HB4(–316) (described above) was used as a probe or competitor.

Semiquantitative Reverse Transcription PCR Analysis

Total RNA was isolated from 5×10^4 cells using a Concert Micro-to-Midi Total RNA Purification System (Invitrogen, Carlsbad, CA, http://www.invitrogen.com). Reverse transcription PCR (RT-PCR) was performed using a SuperScript One-Step RT-PCR system (Invitrogen) according to the manufacturer's instructions with forward/reverse primer sets as follows: c-myc, 5′-CTT CTG CTG GAG GCC ACA GCA AAC CTC CTC and 5′-CCA ACT CCG GGA TCT GGT CAC GCA GGG; $p21^{waf1/cip1}$, 5′-ACA GCA GAG GAA GAC CAT GT and 5′-GGT ATG TAC ATG AGG AGC TG; and β-actin, 5′-GGC GGC AAC ACC ATG TAC CCT and 5′-AGG GGC CGG ACT CGT CAT ACT.

Chromatin Immunoprecipitation Assays

Chromatin immunoprecipitation (ChIP) assays were performed with a ChIP Assay Kit (Upstate, Charlottesville, VA, http://www.upstate.com). Briefly, after transfection with various expression vectors, 293T cells were fixed with 1% formaldehyde. After isolation of nuclear extract, the chromatin was sonicated. Then, protein-DNA complexes were immunoprecipitated with 2 μg of anti-PBX1, anti-HOXB4, or anti-actin Ab. Immunoprecipitated DNA was eluted and subjected to PCR analysis with the following primer pair to amplify 420 bp of the human IGFBP-1 promoter (M59316): forward primer, 5′-GGC ATT

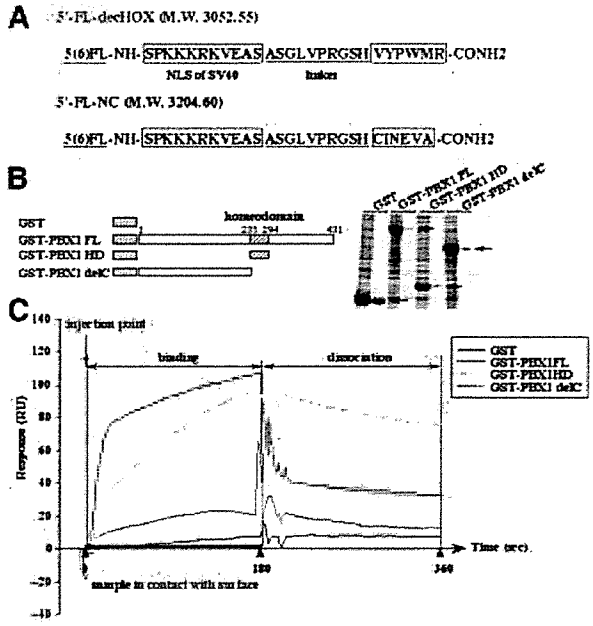

Figure 1. Binding of decHOX to GST-PBX1. **(A):** The structures of the 5′-FL synthetic peptides 5′-FL-decHOX and 5′-FL-NC are indicated. **(B):** GST-PBX1 fusion proteins expressed in *E. coli* were purified by glutathione-Sepharose 4B beads, and their qualities and quantities were confirmed by Coomassie staining. **(C):** In vitro binding of GST-PBX1 to decHOX evaluated by the BIAcore system, with decHOX attached to the sensor chip. To examine the kinetics of the binding and dissociation, various GST-PBX1 proteins were injected onto the sensor chip for 180 seconds and then washed with HEPES-buffered saline for 180 seconds. Abbreviations: decHOX, decoy HOX; delC, C-terminal deletion; FL, fluorescein; GST, glutathione *S*-transferase; HD, homeobox domain; M.W., molecular weight; NC, negative control; NH NLS, nuclear localization signal; RU, resonance unit.

GTT TTC TGC GTT TGA GAA CTG CTG; reverse primer, 5′-CTG GAC ACA GCG CGC ACC TTA TAA AGG GCA. After electrophoresis, PCR products were visualized with ethidium bromide staining.

Statistical Analysis

Data are presented as mean ± SEM or mean ± SD. The statistical significance of the data was determined by the Mann-Whitney *U* test or Student's *t* test. The significance level was set at .05.

RESULTS

The Synthetic Peptide decHOX Binds Directly to the Homeodomain of PBX1

In this study, we attempted to expand CB CD34$^+$ hHSC/HPCs by modifying the function of HOX family proteins. For this purpose, we designed and synthesized a peptide designated decHOX, which was expected to inhibit the interaction between HOX and PBX1. decHOX contains the YPWM motif of HOX, used for its cooperative interaction with PBX1 [36, 37], and the nuclear localization signal (NLS) of the SV40 large T antigen (Fig. 1A) [52]. The negative control (NC) peptide contains the unrelated amino acid sequence CINEVA. To evaluate the efficiency of peptide delivery into CB CD34$^+$ hHSC/HPCs and the subsequent kinetics, FL protein was conjugated to the N termini of both peptides.

First, we examined in vitro binding between decHOX and several GST-PBX1 fusion proteins using the BIAcore system. In this system, the analyte protein is injected onto the sensor chip, the surface of which is covered by the immobilized partner ligand. Binding of the ligand to the analyte is monitored by an increase in arbitrary RUs. Prior to this analysis, we purified several GST-PBX1 fusion proteins (Fig. 1B, left panel) and confirmed their qualities and quantities by Coomassie Brilliant Blue staining (Fig. 1B, right panel). Injection of either GST-full-length PBX1 protein (GST-PBX1 FL) or GST-PBX1 homeobox domain (HD) protein (GST-PBX1 HD) over the decHOX surface resulted in a significant increase in RUs with a lapse of 3 minutes for the binding reaction (Fig. 1C), and these signals increased in a dose-dependent manner (data not shown). In contrast, GST alone and GST-PBX1 delC (lacking the HD) did not bind appreciably to decHOX. After the binding reaction, we injected HEPES-buffered saline for 180 seconds. During this dissociation reaction, GST-PBX1 HD bound to decHOX more stably than GST-PBX1 FL (Fig. 1C). These results suggest that GST-PBX1 FL and GST-PBX1 HD bind to decHOX, probably through HD.

decHOX Can Modulate the Transcriptional Activity of HOX-PBX

To assess the effects of decHOX on HOX-PBX-mediated gene expression, we performed luciferase assays with three types of reporter genes for HOXB4, one containing the c-*myc* promoter (–1,137-c-*myc*-Luc) and the other two containing IGFBP-1 promoters (3 × HB4[–316]-Luc and 3 × HB4[–72]-Luc) as responsive elements, as described previously [49, 53]. Although HOXB4 activated –1,137-c-*myc*-Luc 5.2-fold in 293T cells, PBX1 suppressed this induction (Fig. 2B). However, this inhibitory effect of PBX1 was decreased in a dose-dependent manner by pretreatment with decHOX. Similar responses were observed in assays using 3 × HB4(–316)-Luc and 3 × HB4(–72)-Luc (Fig. 2B). These results indicate that decHOX can enhance the activity of HOXB4 that is suppressed by PBX1.

In a previous study using EMSA, mutant HOX proteins that cannot bind to PBX1 were shown to have defects in DNA-binding activities [39–41]. In contrast, it was reported that the interaction with PBX1 is not necessary for HOXB4 to induce HSC self-renewal [43]. Because decHOX was designed to inhibit the interaction between HOX and PBX1, we evaluated the effect of decHOX on the DNA-binding activity of HOXB4-PBX1 using EMSA. For this purpose, we transfected 293T cells with wild-type (WT) HOXB4 or mutant HOXB4 harboring a WM→AA mutation in the YPWM motif (designated HOXB4 AA; Fig. 2C). Protein(s) in nuclear extracts from 293T cells transfected with PBX1 and HOXB4 WT bound to the HB4(–316) probe (Fig. 2C, lane 2). This band was abolished by WT DNA competitor (Fig. 2C, lane 3) but not by mutant (mt) competitor (Fig. 2C, lane 4), implying that it contains the HOXB4 WT-PBX1 complex. In contrast, proteins in the nuclear extract from HOXB4 AA-transfected cells scarcely bound to the probe, indicating the importance of the YPWM motif for the DNA-binding activity of HOXB4-PBX1 (Fig. 2C, lane 5). Also, pretreatment with decHOX inhibited DNA binding of the HOXB4 WT-PBX1 complex in a dose-

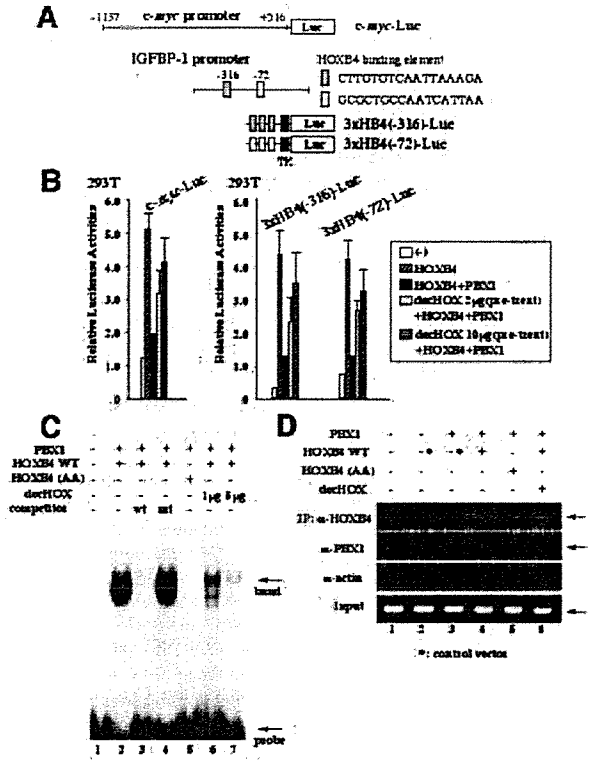

Figure 2. Effects of decHOX on DNA-binding and transcriptional activities of the HOX/PBX complex. **(A):** To construct –1,137-c-*myc*-Luc, a 1,653-base pair fragment of the c-*myc* promoter (–1137 to +516) was subcloned into the plasmid pSP72-Luciferase [47]. To generate 3 × HB4(–316)-Luc and 3 × HB4(–72)-Luc, three tandem repeats of HOXB4-responsive elements in the IGFBP-1 promoter at the indicated locations were subcloned into TK-pGL3 basic-Luc at just upstream of the murine minimal TK promoter linked to the firefly luciferase gene, and their sequences were as indicated. **(B):** 293T cells (2×10^5 cells) seeded in a 60-mm dish were transfected with 6 μg of pcDNA3-HOXB4 alone or in combination with 6 μg of pCS2-PBX1a along with 2 μg of reporter gene and 10 ng of pRL-CMV. After 12 hours, cells were washed, serum-starved for 24 hours, and subjected to luciferase assays using a Dual Luciferase Reporter Assay System. In some experiments, various doses of synthetic peptides were delivered into 293T cells 24 hours prior to luciferase assays. Results are shown as mean ± SD of triplicate cultures. **(C):** 293T cells were transfected with PBX1 together with HOXB4 WT or HOXB4 AA. After 36 hours, nuclear extract was isolated and subjected to electrophoretic mobility shift assay (EMSA) with probes of 3 × HB4(–316). In competition assays, a 200-fold excess of unlabeled wt or mt competitor oligonucleotide was added to the binding mixture. In some experiments, various doses of synthetic peptides were delivered into 293T cells 24 hours prior to EMSA. **(D):** 293T cells transfected with the indicated expression vectors were fixed with 1% formaldehyde. After the isolation of the nuclear extract, chromatin was sonicated. Then, protein-DNA-binding complexes were immunoprecipitated with the 2 μg of the indicated antibodies. Immunoprecipitated DNA was subjected to polymerase chain reaction (PCR) analysis with a primer pair that amplifies 420 base pairs of the human IGFBP-1 promoter. PCR products were electrophoresed onto the agarose gel and visualized with ethidium bromide staining. Abbreviations: decHOX, decoy HOX; IGFBP-1, insulin-like growth factor-binding protein; IP, immunoprecipitation; mt, mutant; WT, wild type.

dependent manner (Fig. 2C, Lanes 6 and 7). These results suggest that decHOX inhibits the interaction between HOXB4 and PBX1 in the ex vivo EMSA binding experiment, thereby suppressing the DNA-binding activity of the HOXB4 WT-PBX1 complex. However, in ChIP assays, which reflect the in vivo DNA-binding state of transcription factors more precisely than EMSA, the HOXB4 AA-PBX1 complex bound to the endogenous IGFBP-1 promoter as efficiently as the HOXB4 WT-PBX1 complex (Fig. 2D, top and second panels, lane 4 vs. lane 5). Also, decHOX barely influenced the DNA-binding activity of the HOXB4 WT-PBX1 complex (Fig. 2D, top and second panels, lane 4 vs. lane 6). Furthermore, we obtained similar results from ChIP assays using two additional primer sets that amplify different sites in the IGFBP-1 promoter (data not shown). From these results, we speculated that HOXB4 is capable of binding to DNA regardless of its interaction with PBX1. However, since we found that PBX1 bound to target DNA in the presence of HOXB4 AA, it is also possible that the YPWM is not required for the interaction between HOXB4 and PBX1. Because the latter speculation is inconsistent with several previous reports indicating the essential role of the YPWM motif in the interaction between HOXB4 and PBX1 [37, 38], further studies using several endogenous promoter sequences will be required to draw a definite conclusion.

decHOX Is Efficiently Delivered into CB CD34$^+$ and Colocalizes with PBX1

Next, we introduced 5′-FL-decHOX into CB CD34$^+$ hHSC/HPCs and analyzed the efficiency of delivery by examining fluorescein intensity with flow cytometry. CD34$^+$ hHSC/HPCs were isolated from CB using AutoMACS and cultured in QBSF-60 serum-free medium containing SCF, FL, TPO, IL-6, and sIL-6R. After culturing for 24 hours, FL-decHOX or FL-NC was delivered into CD34$^+$ cells using the Profect Protein Delivery System. Immediately after delivery (day 0; total culture day 2), 76.2% of CB CD34$^+$ cells were fluorescein-positive (Fig. 3A). Fluorescein intensity decreased with time in culture and was scarcely detectable at day 7. This result suggested that the direct influence of decHOX on CD34$^+$ hHSC/HPCs is limited to 7 days.

Next, we examined the subcellular localizations of PBX1, decHOX, and the NC peptide in hHSC/HPCs using fluorescent microscopy. Forty-eight hours after peptide delivery, both peptides were predominantly detected in the nucleus because of the respective nuclear localization signals. In NC-delivered cells, PBX1 was mainly localized in the cytosol (Fig. 3B, upper panel). On the other hand, in decHOX-delivered cells, PBX1 colocalized with decHOX in the nucleus (Fig. 3B, lower panel). These results suggested that decHOX could interact with PBX1 and colocalized with PBX1 in the nucleus.

decHOX Can Modulate HOX/PBX-Mediated Gene Expression in CB hHSC/HPCs

PBX1 is known to modulate the function of HOX proteins both positively and negatively [30, 32, 33]. For example, HOXB4 induces the expression of c-*myc* in HSCs, and this effect is suppressed by PBX1. On the other hand, HOXA10-mediated expression of $p21^{waf1/cip1}$ is enhanced by PBX1 in myelomonocytic progenitors [28]. To assess the effects of decHOX on the function of HOX proteins in CB cells, we examined the expression of these two target genes. First, to characterize CD34$^+$CD38$^+$ and CD34$^+$CD38$^-$ cells after the ex vivo expansion, we sorted these cells after 9 days in culture and

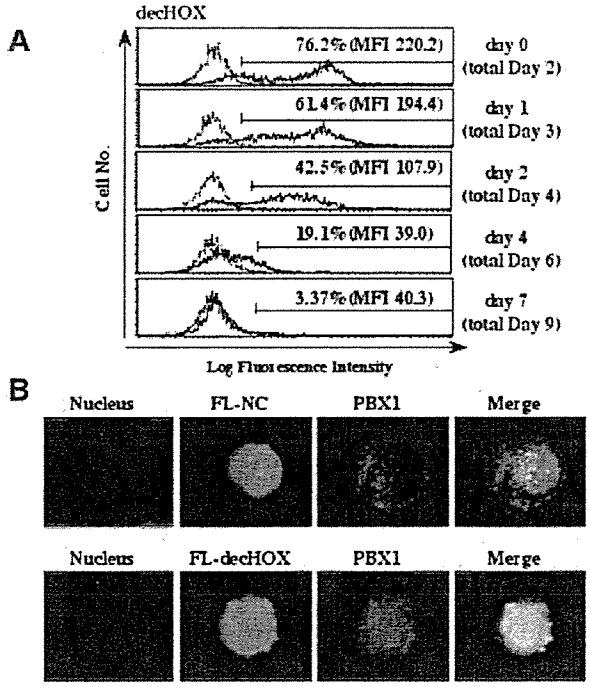

Figure 3. Expression and intracellular localization of decHOX in hHSC/HPCs. **(A):** FL-decHOX was transferred into $CD34^+$ cells by the Profect Protein Delivery System, and fluorescence intensity was assessed by flow cytometry at the indicated times. **(B):** Cytospin preparations of the FL-NC (upper panel)- or FL-decHOX (lower panel)-delivered $CD34^+$ cells were fixed, permeabilized, and incubated with a rabbit anti-human PBX1 antibody (Ab) for 1 hour and then with the anti-rabbit IgG Ab AlexaFluor 546. Cells were rinsed with phosphate-buffered saline containing Hoechst 33342. The stained cells were observed under a confocal laser microscope. Abbreviations: decHOX, decoy HOX; MFI, mean fluorescence intensity; NC, negative control.

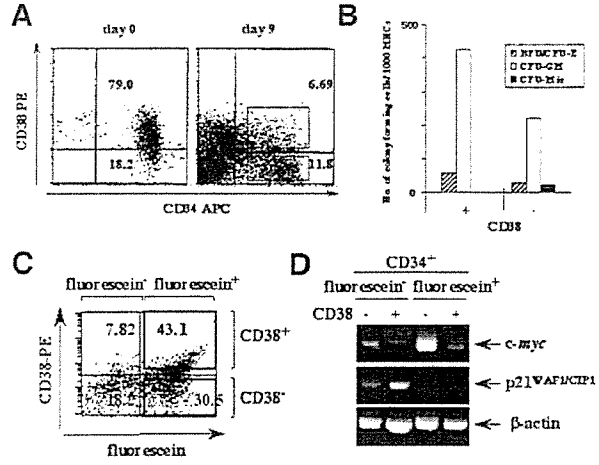

Figure 4. Effects of decoy HOX (decHOX) on target gene expression in hHSC/HPCs. Cord blood (CB) $CD34^+$ cells were cultured in QBSF-60 serum-free medium containing cytokines (stem cell factor, 100 ng/ml; fluorescein [FL], 100 ng/ml; TPO, 10 ng/ml; IL-6, 100 ng/ml; and sIL-6R, 100 ng/ml) for 9 days. **(A):** Before and after culturing, the expression of CD34 and CD38 were examined by flow cytometry. **(B):** After culturing, $CD34^+CD38^-$ and $CD34^+CD38^+$ cells were sorted and subjected to colony assays. **(C):** CB $CD34^+$ cells were treated with FL-decHOX for 48 hours, and then CD38 and fluorescein expression was examined by flow cytometry. **(D):** Cells from each fraction were sorted and subjected to RT-PCR analysis. Abbreviations: APC, allophycocyanin; CFU-GM, colony-forming unit-granulocyte/monocyte precursor; CFU-mix, mixed hematopoietic colony-forming unit.

performed methylcellulose colony assays (Fig. 4A). It was reported that $CD34^+CD38^-$ cells can develop from $CD34^+CD38^+$ cells through the loss of CD38 expression during culturing with cytokines [54]. We found that the primitive colony, mixed hematopoietic colony-forming unit (CFU-Mix) was formed from $CD34^+CD38^-$ cells but not from $CD34^+CD38^+$ cells. Therefore, we supposed that $CD34^+CD38^-$ cells were more primitive than the $CD34^+CD38^+$ cells that developed after ex vivo culturing. Next, we treated CB $CD34^+$ cells with 5′-FL-decHOX, cultured for 48 hours, and subjected them to flow cytometric analysis. At that point, 43.1% of the cultured cells were $fluorescein^+CD38^+$, 30.5% were $fluorescein^+CD38^-$, 7.82% were $fluorescein^-CD38^+$, and 18.2% were $fluorescein^-CD38^-$ (Fig. 4C). Then, we sorted the cells from each fraction and subjected them to semiquantitative RT-PCR analysis. In the $CD34^+CD38^-$ immature cell fraction, c-*myc* expression was increased in the decHOX-delivered $fluorescein^+$ fraction compared with the $fluorescein^-$ control fraction (Fig. 4D, top panel, lane 1 vs. lane 3). Conversely, in the $CD34^+CD38^+$ mature fraction, the expression of $p21^{waf1/cip1}$ was decreased in the $fluorescein^+$ fraction compared with the $fluorescein^-$ fraction (Fig. 4D, middle panel, lane 2 vs. lane 4). Together, these results suggest that decHOX binds to PBX1 as a HOX decoy and cancels both the positive and negative effects of PBX1 on HOX proteins in $CD34^+$ hHSC/HPCs.

decHOX Enhances Cytokine-Dependent Ex Vivo Expansion of CB hHSC/HPCs

Next, we examined effects of decHOX on the growth and differentiation of CB $CD34^+$ hHSC/HPCs. As shown in Figure 5, purified $CD34^+$ cells were exposed to 5′-FL-decHOX or 5′-FL-NC for 24 hours. Then, 1×10^4 $fluorescein^+$ cells were sorted and cultured in QBSF-60 serum-free medium containing SCF, FL, TPO, IL-6, and sIL-6R for 7 days, during which, medium dilution was performed as indicated. After these cultures, no apparent difference was observed between the total number of viable decHOX-treated and NC-treated cells (Fig. 6A). However, the proportion of $CD34^+$ cells was significantly higher in decHOX-treated cells than in NC-treated cells (decHOX, 33.2%; NC, 17.9%) (Fig. 6B). Similar results were obtained from five independent experiments (data not shown). Accordingly, the fold expansion of $CD34^+$ cells was higher in decHOX-delivered cells than in NC-delivered cells (decHOX, 32.5 ± 8.71-fold; NC, 17.2 ± 6.25-fold [$n = 6$] [$p < .05$]) (Fig. 6A). Furthermore, cultures treated with decHOX retained immature cells with $CD34^+CD38^-$ or $CD45^+HLA\text{-}DR^-$ phenotype more effectively than NC-treated cells (percentage $CD34^+CD38^-$ cells: decHOX, 24.2% ± 6.67%; NC, 14.8% ± 6.17% [$n = 3$] [$p < .05$]; percentage $CD45^+HLA\text{-}DR^-$ cells: decHOX, 37.2% ± 6.98%; NC, 18.8% ± 7.44% [$n = 3$] [$p < .05$]) (representative results from one experiment are shown in Fig. 6B). To characterize the ex vivo expanded cells, we ana-

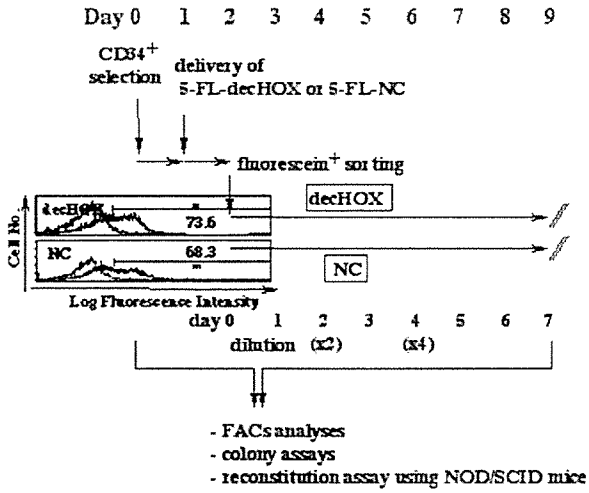

Figure 5. Experimental design. $CD34^+$ hematopoietic stem/progenitor cells were isolated from cord blood and cultured in serum-free medium containing cytokines. FL-decHOX or FL-NC was then delivered into $CD34^+$ cells. Twenty-four hours after peptide delivery, approximately 70% of cultured cells were fluorescein-positive. Fluorescein-positive cells were sorted and cultured for 7 days. Medium dilutions were performed as indicated. Cultured cells were then subjected to FACS analyses, colony assays, and reconstitution assays using NOD/SCID mice. Abbreviations: decHOX, decoy HOX; FACS, fluorescence-activated cell sorting; FL, fluorescein; NC, negative control.

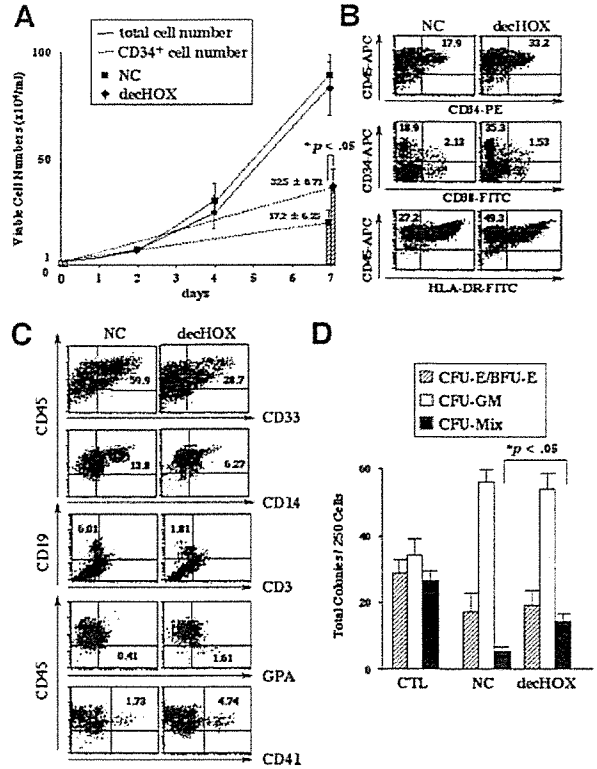

Figure 6. Effects of decHOX on biological properties and functions of hHSC/HPCs cultured with cytokines. After treatment with fluorescein (FL)-decHOX or FL-NC, fluorescein-positive cells were sorted and cultured for 7 days. **(A):** The total number of viable cells and their surface phenotypes were examined. Results are shown as mean ± SD ($n = 6$). **(B, C):** Representative fluorescence-activated cell sorting data from one experiment are shown. **(D):** Cultured cells were subjected to methylcellulose colony assays using freshly isolated cells as a control. All cultures were done in triplicate and scored after 10 days. Results are shown as mean ± SD ($n = 4$). Abbreviations: BFU-E, burst-forming unit-erythroid precursor; CFU-E, colony-forming unit-erythrocyte precursor; CFU-GM, colony-forming unit-granulocyte/monocyte precursor; CFU-Mix, mixed hematopoietic colony-forming unit; CTL, control; decHOX, decoy HOX; FITC, fluorescein isothiocyanate; HLA, human leukocyte antigen; NC, negative control; PE, phycoerythrin.

lyzed the expression of lineage markers on these cells (Fig. 6C). Fluorescence-activated cell sorting analyses after 7 days in culture indicated that both NC- and decHOX-treated cells contained not only immature cells but also mature cells expressing lineage markers such as CD33 (myeloid), CD14 (monocytic), CD19 (B lymphoid), GPA (erythroid), and CD41 (megakaryocytic). Except for GPA and CD41 expression, the expression of these markers was notably lower in decHOX-delivered cells than in NC-delivered cells. Next, we analyzed the effects of decHOX on colony-forming activities of CB $CD34^+$ hHSC/HPCs. As shown in Figure 6D, both decHOX- and NC-delivered cells, which contain approximately 33% and 18% of $CD34^+$ cells, respectively (Fig. 6B), generated all types of colonies, and the numbers of colony-forming unit-erythrocyte precursor/burst-forming unit-erythroid precursor and colony-forming unit-granulocyte/monocyte precursor colonies were nearly the same in both cultures. However, decHOX more effectively yielded CFU-Mix primitive colonies than NC (CFU-Mix colonies per 250 cultured cells: decHOX, 15.3 ± 2.1; NC, 7.5 ± 0.8 [$n = 6$] [$p < .05$]). Together, these results suggest that although both immature progenitors and mature cells were amplified during culturing, decHOX selectively expands immature progenitors.

decHOX-Treated hHSC/HPCs Reconstitute Hematopoiesis Rapidly and Efficiently in NOD/SCID Mice

Next, we assessed the effects of decHOX on engrafting abilities of CB $CD34^+$ hHSC/HPCs by xenotransplantation into NOD/SCID mice. For this purpose, 2×10^4 CB $CD34^+$ cells were treated with decHOX or NC and cultured in QBSF-60 containing cytokines for 7 days. Then, total cultured cells were transplanted into NOD/SCID mice that were treated with 2.4 Gy of TBI and i.p. injection of anti-asialo-GM1 Ab immediately before and after transplantation (days 7 and 14) (each group, $n = 9$). Also, 2×10^4 freshly isolated CB $CD34^+$ cells derived from the same sample as the expanded cells were transplanted as a control (CTL). CTL cells are expected to contribute to hematopoiesis in approximately 10% of BM cells after 4 weeks under our experimental conditions using NOD/SCID mice. When decHOX-treated cells were transplanted, human $CD45^+$ ($hCD45^+$) cells constituted 9.17% of the BM cells 4 weeks after transplantation, whereas NC-treated cells yielded only 4.28% $hCD45^+$ cells (Fig. 7A). In addition, the proportion of $hCD34^+$ cells in the BM was increased by decHOX (decHOX, 3.05%; NC, 1.22%) (Fig. 7A). We also analyzed the lineage distributions of $hCD45^+$ cells in BM of mice that received transplants of decHOX-treated cells at 4 and 8 weeks after transplantation.

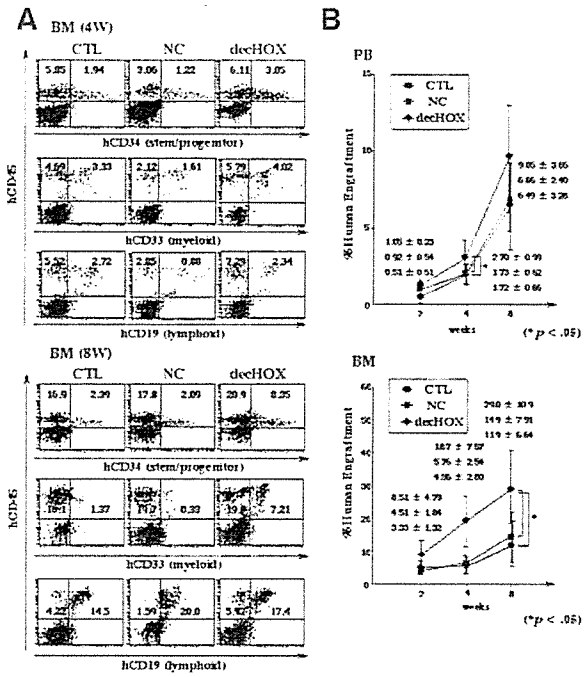

Figure 7. Xenotransplantation into nonobese diabetic/severe combined immunodeficient (NOD/SCID) mice. **(A):** A total of 2×10^4 decHOX- or NC-delivered cells were sorted and subjected to the culture for 7 days. Whole expanded cells or 2×10^4 freshly isolated $CD34^+$ cells were transplanted into 5–6-week-old NOD/SCID mice subjected to immunosuppressive treatment before and after transplantation (each group, n = 9). Four weeks after transplantation, the proportion of engrafted human cells in BM was assessed by flow cytometry with anti-hCD45-PE antibody (Ab). Four weeks and 8 weeks after transplantation, short-term repopulation abilities of the ex vivo-expanded cells were analyzed using BM and PB cells with the indicated Abs. Representative flow cytometry data obtained from BM cells are shown. **(B):** Kinetics of engraftment in PB and BM of NOD/SCID mice are indicated. Results are shown as mean ± SD (each group, n = 9). Abbreviations: BM, bone marrow; CTL, control; decHOX, decoy HOX; NC, negative control; PB, peripheral blood; PE, phycoerythrin; W, weeks.

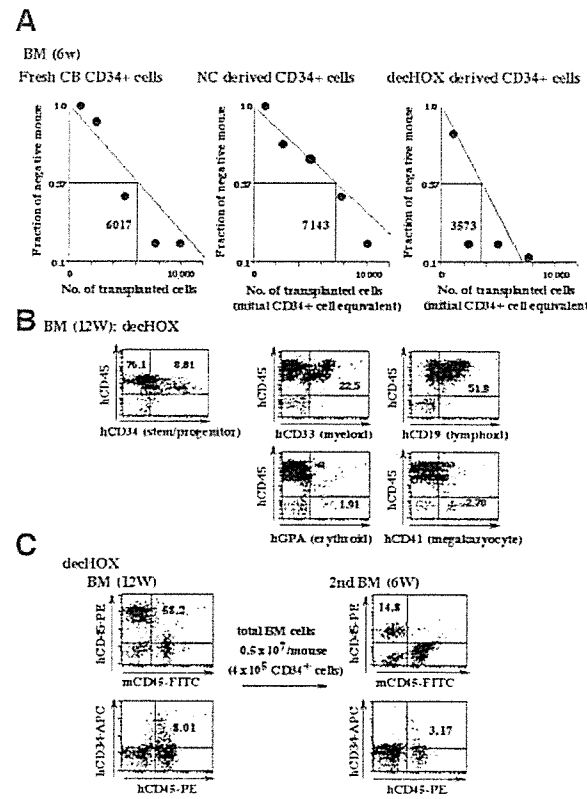

Figure 8. Long-term repopulating abilities in decHOX-delivered cells. **(A):** Frequencies of human HSCs capable of repopulating in nonobese diabetic/severe combined immunodeficient (NOD/SCID) mice in freshly isolated CB $CD34^+$ cells (n = 26), NC-treated cells (n = 29), and decHOX-treated cells (n = 23) were quantified by limiting dilution analyses. **(B):** Twelve weeks after transplantation, the long-term repopulating ability of the decHOX-treated cells was analyzed by flow cytometry using BM from NOD/SCID mouse highly reconstituted with human cells. **(C):** Twelve weeks after transplantation, BM cells were isolated from NOD/SCID mice that received transplants of decHOX-treated cells and injected into secondary recipients (n = 5). Six weeks after transplantation, the proportions of engrafted human cells in BM were assessed by flow cytometry. Representative data are shown. Abbreviations: BM, bone marrow; CB, cord blood; decHOX, decoy HOX; FITC, fluorescein isothiocyanate; hCD, human cluster of differentiation; NC, negative control; PE, phycoerythrin; W, weeks.

As shown in Figure 7A, transplanted decHOX-treated cells not only retained $CD34^+$ cells but also generated $CD33^+$ myeloid cells and $CD19^+$ B cells more effectively than CTL and NC-treated cells.

We also analyzed the kinetics of short-term repopulation in the PB and BM of recipient mice. Two weeks after transplantation, $hCD45^+$ cells were detectable in both BM and PB without significant differences in their frequencies among decHOX, NC, and CTL groups (Fig. 7B). However, at 4 weeks, the proportion of $hCD45^+$ cells in PB was significantly higher in the decHOX group than in the NC and CTL groups (decHOX, 2.70% ± 0.36%; NC, 1.73% ± 0.14%; CTL, 1.72% ± 0.16%) ($p < .05$). This result suggests that decHOX reduces the delay in engraftment associated with CB transplantation (Fig. 7B). Also, the percentage of $hCD45^+$ cells in BM was significantly higher in the decHOX group than in the CTL and NC groups at 8 weeks (decHOX, 29.0% ± 10.9%; CTL, 11.9% ± 6.64%; NC, 14.9% ± 7.91% [$p < .05$]).

Given the possibility that decHOX supports the expansion of long-term repopulating (LTR)-HSCs, we next calculated the expansion rate using a limiting dilution method. To obtain the highest possible levels of human cell engraftment, recipient mice were treated with TBI in combination with anti-asialo GM1 Ab immediately before and after transplantation (days 7, 14, 21, and 28). As shown in Figure 8A, the frequency of LTR-HSCs was calculated to be 1 in 6,017 freshly isolated CB $CD34^+$ cells and 1 in 7,143 NC-treated cells. In contrast, the frequency of LTR-HSCs in decHOX-treated cells was calculated to be 1 in 3,573. Accordingly, the expansion of LTR-HSCs by decHOX was estimated to be 2.0-fold. Furthermore, in BM highly reconstituted with decHOX-treated human cells, we detected considerable proportions of $hCD45^+CD33^+$ cells (22.5%) and $hCD45^+hCD19^+$ cells (51.8%) 12 weeks after transplantation. In addition, $hCD45^+CD34^+$ cells were an estimated 8.81% of total BM cells (Fig. 8B).

To further examine the long-term reconstituting activity of decHOX-treated cells, we performed a secondary transplantation. Twelve weeks after the first transplantation, we isolated BM cells from two mice that received transplants of decHOX-treated cells. A mixture of these cells (58.2% and 8.0% of which were $hCD45^+$ and $hCD34^+$, respectively) was transplanted into five recipients at 4.0×10^5 $hCD34^+$ cells per mouse. An apparent second engraftment was detected in the BM of 2 of 5 mice 6 weeks after the transplantation (representative data are shown in Fig. 8C). At this point, $hCD45^+$ cells were an estimated 14.8% of the total BM cells in the recipient mouse. Furthermore, approximately 20% of $hCD45^+$ cells expressed CD34 (3.17% of total BM cells). Taken together, these results indicate that CB $CD34^+$ hHSCs/HPCs expanded by decHOX reconstitute hematopoiesis more rapidly and efficiently than control cells, and these cells have long-term reconstituting abilities in NOD/SCID mice.

DISCUSSION

HOXB4-deficient mice do not exhibit obvious abnormalities in hematopoiesis except for a minor proliferative defect of HSCs detected by reconstitution assays, suggesting that HOXB4 is dispensable for normal hematopoiesis [55]. It was speculated that HOXB4 functional roles can be replaced by other HOX family members because mice lacking both HOXB4 and HOXB3 had more apparent defects in hematopoiesis than those lacking HOXB4 alone [56]. However, HOXB4 has attracted particular interest during the last few years because its gene transfer induced ~40-fold murine and ~30-fold human HSC expansion ex vivo, suggesting possible clinical applications [16, 21]. Regarding clinical use, there was an initial concern that constitutive expression of HOXB4 in HSCs might cause leukemia. This is because deregulated expression of HOXB8 was found in myeloid leukemia, and HOX family genes are sometimes involved in leukemogenic chromosomal translocations, such as t(7,11)(p15;p15), yielding NUP98-HOXA9 [57, 58]. However, HSCs expanded by HOXB4 treatment reconstituted all hematopoietic lineages in mice that received transplants mice without causing leukemia, indicating that HSCs expressing HOXB4 were regulated by the hematopoietic system [16]. To eliminate any deleterious effects caused by stable HOXB4 gene transfer, Krosl et al. tried to expand murine HSCs by delivering HOXB4 protein [20]. In that study [20], cell membrane-permeable, recombinant TAT-HOXB4 protein was added to the culture medium, inducing a fivefold net expansion of HSCs. Although TAT-HOXB4 was supposed to be delivered with high efficiency, its half-life was estimated to be only 1 hour. In addition, Amsellem et al. tried to expand human CB HSCs using HOXB4 protein [19]. They used HOXB4 protein secreted into the culture supernatant from cocultured MS-5 murine stromal cells, and this approach increased NOD/SCID mouse repopulating cells (SRCs) 2.5-fold. However, the efficiency of protein delivery was not very high, and the coculture system may not be practical for clinical applications. In contrast, our decHOX could be delivered into more than 70% of CB $CD34^+$ hHSC/HPCs and was detected in these cells even after 4 days.

Because similar decoy peptides, such as NFAT and JNK-interacting-protein-1 (JIP-1) decoy peptides were shown to be harmless at the genomic level [59, 60], decHOX may be useful for clinical applications. Furthermore, it is possible to use decHOX in combination with HOX proteins [19, 20] to further augment the activity of HOXB4. However, it should be noted that Brun et al. reported that an excessive amount of HOXB4 introduced by an adenoviral vector system inhibits self-renewal of human CB HSCs and induces myeloid differentiation [22]. Therefore, it is necessary to determine the optimal amount of HOXB4 for enforcing HSC self-renewal.

Recently, DiMartino et al. generated Pbx1-null mice, which died at embryonic day 15 or 16 due to anemia, and reported that PBX1 is required for the maintenance of definitive hematopoiesis and contributes to the mitotic amplifications of progenitor subsets [61]. However, Krosl et al. demonstrated that antisense DNA against PBX1 apparently augmented self-renewal of HSCs overexpressing HOXB4 but was not effective on normal HSCs, suggesting that PBX1 may be a negative regulator of HOXB4-mediated self-renewal of HSCs [42]. In accordance with this result, we found that decHOX could enhance cytokine-mediated self-renewal of HSCs by modifying the function of HOXB4. Furthermore, we found that decHOX restored HOXB4 activity suppressed by PBX1 without affecting DNA-binding activities. The interaction between the YPWM motif in HOX and the homeodomain in PBX1 modifies the DNA-binding affinities of the proteins and their coactivator/corepressor binding-dependent transcriptional activities, and decHOX presumably affects the latter interactions. At present, we know that decHOX can augment HOXB4-dependent transcription of c-*myc*, which we recently identified as a key regulator of HOXB4- and Notch1-mediated HSC self-renewal [49]. However, HOX-PBX complexes regulate a number of genes in HSCs both positively and negatively. Also, PBX1 shows dual (positive and negative) effects on HOX-mediated transcription according to the target genes and/or the cellular context [31, 33, 34]. Thus, further studies to identify the target genes of HOX/PBX1 in HSCs would provide useful information to facilitate decHOX-mediated ex vivo amplification of HSCs.

To date, two groups of investigators have used ex vivo-amplified CB HSCs for transplantation. Shpall et al. [5] isolated $CD34^+$ cells from CB. Forty percent of the isolated cells were expanded in medium containing SCF, G-CSF, and TPO for 10 days, and the remaining 60% were immediately transplanted or stored frozen until transplantation. After high-dose chemotherapy, 37 patients (25 adults, 12 children) received transplants of expanded $CD34^+$ cells and nonexpanded cells with a median dose of 0.99×10^7 nucleated cells per kilogram. The median time to engraftment of neutrophils (neutrophil count $> 500/\mu l$) was 28 days (range, 15–49 days) and that of platelets (platelet $> 20{,}000/\mu l$) was 106 days (range, 38–345 days). The authors of that study concluded that although the ex vivo expansion of CB cells was feasible and safe, expanded HSCs did not improve the time to engraftment in recipients [5]. In a phase I trial, Jaroscak et al. [6] transplanted CB HSCs expanded by PIXY321, FL, and EPO into 28 patients with a median dose of 2.4×10^7 nucleated cells per kilogram. They also concluded that the ex vivo expanded CB HSCs were not effective in shortening the recovery period [6]. In contrast, the present study showed that decHOX can expand short-term as well as long-term SRC, thereby shortening the delay in hematopoietic recovery, suggesting that decHOX may be an effective tool to resolve this problem. Since HSC quiescence is regulated by $p21^{waf1/cip1}$, $p16^{INK4A}$, and

$p18^{INK4C}$ and progenitor quiescence by $p27^{kip2}$ [62–66], a basic study focusing on the expression of cell cycle control molecules in decHOX-transduced cells may clarify the mechanism of decHOX-mediated rapid recovery of hematopoiesis.

In conclusion, in the present study we demonstrated that decHOX can further augment cytokine-mediated ex vivo expansion of CB HSCs and that these expanded HSCs can restore hematopoiesis more rapidly and effectively than freshly prepared CB HSCs. However, it is necessary to further optimize treatment conditions, such as the method and timing of peptide delivery. Also, to enhance the effects of decHOX, it will be useful to explore the combined effects of other signals that can support HSC self-renewal, such as SHH and Wnt. We hope that our decHOX will eventually benefit patients with hematopoietic malignancies.

ACKNOWLEDGMENTS

We are grateful to N. Takada, K. Maruyama, and M. Hirose for technical support and animal care and Y. Ikegami for laboratory management. This work was supported by grants from the Ministry of Health, Labour and Welfare of Japan (number 18790672, to N.T.), Uehara Foundation (to K.Y.), and Hovansha Foundation (to K.Y.).

DISCLOSURES

The authors indicate no potential conflicts of interest.

REFERENCES

1 Benito AI, Diaz MA, Gonzalez-Vicent M et al. Hematopoietic stem cell transplantation using umbilical cord blood progenitors: Review of current clinical results. Bone Marrow Transplant 2004;33:675–690.

2 Devine SM, Lazarus HM, Emerson SG. Clinical application of hematopoietic progenitor cell expansion: Current status and future prospects. Bone Marrow Transplant 2003;31:241–252.

3 Heike T, Nakahata T. Ex vivo expansion of hematopoietic stem cells by cytokines. Biochim Biophys Acta 2002;1592:313–321.

4 Ueda T, Tsuji K, Yoshino H et al. Expansion of human NOD/SCID-repopulating cells by stem cell factor, Flk2/Flt3 ligand, thrombopoietin, IL-6, and soluble IL-6 receptor. J Clin Invest 2000;105:1013–1021.

5 Shpall EJ, Quinones R, Giller R et al. Transplantation of ex vivo expanded cord blood. Biol Blood Marrow Transplant 2002;8:368–376.

6 Jaroscak J, Goltry K, Smith A et al. Augmentation of umbilical cord blood (UCB) transplantation with ex vivo-expanded UCB cells: Results of a phase 1 trial using the AastromReplicell System. Blood 2003;101: 5061–5067.

7 Brandon C, Eisenberg LM, Eisenberg CA. WNT signaling modulates the diversification of hematopoietic cells. Blood 2000;96:4132–4141.

8 Murdoch B, Chadwick K, Martin M et al. Wnt-5A augments repopulating capacity and primitive hematopoietic development of human blood stem cells in vivo. Proc Natl Acad Sci U S A 2003;100:3422–3427.

9 Reya T, Duncan AW, Ailles L et al. A role for Wnt signalling in self-renewal of haematopoietic stem cells. Nature 2003;423:409–414.

10 Willert K, Brown JD, Danenberg E et al. Wnt proteins are lipid-modified and can act as stem cell growth factors. Nature 2003;423:448–452.

11 Bhatia M, Bonnet D, Wu D et al. Bone morphogenetic proteins regulate the developmental program of human hematopoietic stem cells. J Exp Med 1999;189:1139–1148.

12 Bhardwaj G, Murdoch B, Wu D. Sonic hedgehog induces the proliferation of primitive human hematopoietic cells via BMP regulation. Nat Immunol 2001;2:178–180.

13 Varnum-Finney B, Xu L, Brashem-Stein C et al. Pluripotent, cytokine-dependent, hematopoietic stem cells are immortalized by constitutive Notch1 signaling. Nat Med 2000:6:1278–1281.

14 Karanu FN, Murdoch B, Gallacher L et al. The notch ligand jagged-1 represents a novel growth factor of human hematopoietic stem cells. J Exp Med 2000;192:1365–1372.

15 Ohishi K, Varnum-Finney B, Bernstein ID. Delta-1 enhances marrow and thymus repopulating ability of human CD34(+)CD38(–) cord blood cells. J Clin Invest 2002;110:1165–1174.

16 Antonchuk J, Sauvageau G, Humphries RK. HOXB4-induced expansion of adult hematopoietic stem cells ex vivo. Cell 2002;109:39–45.

17 Lessard J, Sauvageau G. Bmi-1 determines the proliferative capacity of normal and leukaemic stem cells. Nature 2003;423:255–260.

18 Park IK, Qian D, Kiel M et al. Bmi-1 is required for maintenance of adult self-renewing haematopoietic stem cells. Nature 2003;423:302–305.

19 Amsellem S, Pflumio F, Bardinet D et al. Ex vivo expansion of human hematopoietic stem cells by direct delivery of the HOXB4 homeoprotein. Nat Med 2003;9:1423–1427.

20 Krosl J, Austin P, Beslu N et al. In vitro expansion of hematopoietic stem cells by recombinant TAT-HOXB4 protein. Nat Med 2003;9:1428–1432.

21 Buske C, Feuring-Buske M, Abramavich C et al. Deregulated expression of HOXB4 enhances the primitive growth activity of human hematopoietic cells. Blood 2002;100:862–868.

22 Brun AC, Fan X, Bjornsson JM et al. Enforced adenoviral vector-mediated expression of HOXB4 in human umbilical cord blood CD34+ cells promotes myeloid differentiation but not proliferation. Mol Ther 2003;8:618–628.

23 Magli MC, Largman C, Lawrence HJ. Effects of HOX homeobox genes in blood cell differentiation. J Cell Physiol 1997;173:168–177.

24 Buske C, Humphries RK. Homeobox genes in leukemogenesis. Int J Hematol 2000;71:301–308.

25 Lawrence HJ, Helgason CD, Sauvageau G et al. Mice bearing a targeted interruption of the homeobox gene HOXA9 have defects in myeloid, erythroid, and lymphoid hematopoiesis. Blood 1997;89: 1922–1930.

26 Dorsam ST, Ferrell CM, Dorsam GP et al. The transcriptome of the leukemogenic homeoprotein HOXA9 in human hematopoietic cells. Blood 2004;103:1676–1684.

27 Crooks GM, Fuller J, Petersen D et al. Constitutive HOXA5 expression inhibits erythropoiesis and increases myelopoiesis from human hematopoietic progenitors. Blood 1999;94:519–528.

28 Bromleigh VC, Freedman LP. p21 is a transcriptional target of HOXA10 in differentiating myelomonocytic cells. Genes Dev 2000; 14:2581–2586.

29 Bjornsson JM, Andersson E, Lundstrom P et al. Proliferation of primitive myeloid progenitors can be reversibly induced by HOXA10. Blood 2001;98:3301–3308.

30 Zimmermann F, Rich IN. Mammalian homeobox B6 expression can be correlated with erythropoietin production sites and erythropoiesis during development, but not with hematopoietic or nonhematopoietic stem cell populations. Blood 1997:89:2723–2735.

31 Mann RS, Affolter M. Hox proteins meet more partners. Curr Opin Genet Dev 1998:8:423–429.

32 Pineault N, Helgason CD, Lawrence HJ et al. Differential expression of Hox, Meis1, and Pbx1 genes in primitive cells throughout murine hematopoietic ontogeny. Exp Hematol 2002;30:49–57.

33 Di Rocco G, Mavilio F, Zappavigna V. Functional dissection of a transcriptionally active, target-specific Hox-Pbx complex. EMBO J 1997;16:3644–3654.

34 Asahara H, Dutta S, Kao HY et al. Pbx-Hox heterodimers recruit coactivator-corepressor complexes in an isoform-specific manner. Mol Cell Biol 1999;19:8219–8225.

35 Saleh M, Rambaldi I, Yang XJ et al. Cell signaling switches HOX-PBX complexes from repressors to activators of transcription mediated by histone deacetylases and histone acetyltransferases. Mol Cell Biol 2000; 20:8623–8633.

36 Lu Y, Goldenberg I, Bei L et al. HoxA10 represses gene transcription in undifferentiated myeloid cells by interaction with histone deacetylase 2. J Biol Chem 2003;278:47792–47802.

37 Phelan ML, Rambaldi I, Featherstone MS. Cooperative interactions between HOX and PBX proteins mediated by a conserved peptide motif. Mol Cell Biol 1995;15:3989–3997.

38 Piper DE, Batchelor AH, Chang CP et al. Structure of a HoxB1-Pbx1 heterodimer bound to DNA: Role of the hexapeptide and a fourth homeodomain helix in complex formation. Cell 1999;96:587–597.

39 Shanmugam K, Featherstone MS, Saragovi HU. Residues flanking the HOX YPWM motif contribute to cooperative interactions with PBX. J Biol Chem 1997;272(30):19081–19087.

40 Sprules T, Green N, Featherstone M et al. Conformational changes in the PBX homeodomain and C-terminal extension upon binding DNA and HOX-derived YPWM peptides. Biochemistry 2000;39:9943–9950.

41 LaRonde-LeBlanc NA, Wolberger C. Structure of HoxA9 and Pbx1 bound to DNA: Hox hexapeptide and DNA recognition anterior to posterior. Genes Dev 2003;17:2060–2072.

42 Krosl J, Beslu N, Mayotte N et al. The competitive nature of HOXB4-transduced HSC is limited by PBX1: the generation of ultra-competitive stem cells retaining full differentiation potential. Immunity 2003;18:561–571.

43 Beslu N, Krosl J, Laurin M et al. Molecular interactions involved in HOXB4-induced activation of HSC self-renewal. Blood 2004;104: 2307–2314.

44 Tanaka H, Matsumura I, Ezoe S et al. E2F1 and c-Myc potentiate apoptosis through inhibition of NF-kappaB activity that facilitates Mn-SOD-mediated ROS elimination Mol Cell 2002;9:1017–1029.

45 Cannon MJ, Papalia GA, Navratilova I et al. Comparative analyses of a small molecule/enzyme interaction by multiple users of Biacore technology. Anal Biochem 2004;330:98–113.

46 Tajima S, Tsuji K, Ebihara Y et al. Analysis of interleukin 6 receptor and gp130 expressions and proliferative capability of human CD34+ cells. J Exp Med 1996;184:1357–1364.

47 Bhatia M, Bonnet D, Kapp U et al. Quantitative analysis reveals expansion of human hematopoietic repopulating cells after short-term ex vivo culture. J Ex Med 1997;186:619–624.

48 Wang JC, Doedens M, Dick JE. Primitive human hematopoietic cells are enriched in cord blood compared with adult bone marrow or mobilized peripheral blood as measured by the quantitative in vivo SCID-repopulating cell assay. Blood 1997;89:3919–3924.

49 Satoh Y, Matsumura I, Tanaka H et al. Roles for c-Myc in self-renewal of hematopoietic stem cells. J Biol Chem 2004;279:24986–24993.

50 Matsumura I, Kitamura T, Wakao H et al. Transcriptional regulation of the cyclin D1 promoter by STAT5: its involvement in cytokine-dependent growth of hematopoietic cells. EMBO J 1999;18:1367–1377.

51 Matsumura I, Ishikawa J, Nakajima K et al. Thrombopoietin-induced differentiation of a human megakaryoblastic leukemia cell line, CMK, involves transcriptional activation of p21(WAF1/Cip1) by STAT5. Mol Cell Biol 1997;17:2933–2943.

52 Hodel MR, Corbett AH, Hodel AE. Dissection of a nuclear localization signal. J Biol Chem 2001;276:1317–1325.

53 Gao J, Mazella J, Tseng L. Hox proteins activate the IGFBP-1 promoter and suppress the function of hPR in human endometrial cells. DNA Cell Biol 2002;21:819–825.

54 Dorrell C, Gan OI, Pereira DS et al. Expansion of human cord blood CD34(+)CD38(–) cells in ex vivo culture during retroviral transduction without a corresponding increase in SCID repopulating cell (SRC) frequency: Dissociation of SRC phenotype and function. Blood 2000;95: 102–110.

55 Brun AC, Bjornsson JM, Magnusson M et al. Hoxb4-deficient mice undergo normal hematopoietic development but exhibit a mild proliferation defect in hematopoietic stem cells. Blood 2004;103:4126–4133.

56 Björnsson JM, Larsson N, Brun AC et al. Reduced proliferative capacity of hematopoietic stem cells deficient in Hoxb3 and Hoxb4. Mol Cell Biol 2003;23:3872–3883.

57 Knoepfler PS, Sykes DB, Pasillas M et al. HoxB8 requires its Pbx-interaction motif to bl7ck differentiation of primary myeloid progenitors and of most cell line models of myeloid differentiation. Oncogene 2001;20:5440–5448.

58 Kroon E, Thorsteinsdottir U, Mayotte N et al. NUP98-HOXA9 expression in hemopoietic stem cells induces chronic and acute myeloid leukemias in mice. EMBO J 2001;20:350–361.

59 Noguchi H, Matsushita M, Okitsu et al. A new cell-permeable peptide allows successful allogeneic islet transplantation in mice. Nat Med 2004;10:305–309.

60 Kaneto H, Nakatani Y, Miyatsuka T et al. Possible novel therapy for diabetes with cell-permeable JNK-inhibitory peptide. Nat Med 2004;10: 1128–1132.

61 DiMartino JF, Selleri L, Traver D et al. The Hox cofactor and proto-oncogene Pbx1 is required for maintenance of definitive hematopoiesis in the fetal liver. Blood 2001;98:618–626.

62 Furukawa U, Kikuchi J, Nakamura M et al. Lineage-specific regulation of cell cycle control gene expression during haematopoietic cell differentiation. Br J Haematol 2000;110:663–673.

63 Cheng T, Rodrigues N, Shen H et al. Hematopoietic stem cell quiescence maintained by p21cip1/waf1. Science 2000;287:1804–1808.

64 Yuan Y, Shen H, Franklin DS et al. In vivo self-renewing divisions of haematopoietic stem cells are increased in the absence of the early G1-phase inhibitor, p18INK4C. Nat Cell Biol 2004;6:436–442.

65 Ito K, Hirao A, Arai F et al. Regulation of oxidative stress by ATM is required for self-renewal of haematopoietic stem cells. Nature 2004;431: 997–1002.

66 Cheng T, Rodrigues N, Dombkowski D et al. Stem cell repopulation efficiency but not pool size is governed by p27(kip1). Nat Med 2000;6: 1235–1240.

HOX Decoy Peptide Enhances the Ex Vivo Expansion of Human Umbilical Cord Blood CD34 + Hematopoietic Stem Cells/Hematopoietic Progenitor Cells

Hirokazu Tanaka, Itaru Matsumura, Kiminari Itoh, Asako Hatsuyama, Masayuki Shikamura, Yusuke Satoh, Toshio Heike, Tatsutoshi Nakahata and Yuzuru Kanakura

Stem Cells 2006;24;2592-2602
DOI: 10.1634/stemcells.2005-0434

bjh short report

Preceding immunosuppressive therapy with antithymocyte globulin and ciclosporin increases the incidence of graft rejection in children with aplastic anaemia who underwent allogeneic bone marrow transplantation from HLA-identical siblings

Ryoji Kobayashi,[1] Hiromasa Yabe,[2] Junichi Hara,[3] Akira Morimoto,[4] Masahiro Tsuchida,[5] Hideo Mugishima,[6] Akira Ohara,[7] Ichiro Tsukimoto,[8] Koji Kato,[9] Hisato Kigasawa,[10] Ken Tabuchi,[10] Tatsutoshi Nakahata,[11] Shoichi Ohga[12] and Seiji Kojima[13]: the Japan Childhood Aplastic Anemia Study Group

[1]Department of Paediatrics, Hokkaido University Graduate School of Medicine, Sapporo, Japan, [2]Specialized Clinical Science, Pediatrics, Tokai University School of Medicine, Isehara, Japan, [3]Department of Paediatrics, Osaka City Central Hospital, Osaka, Japan, [4]Department of Paediatrics, Kyoto Prefectural University of Medicine, Graduate School of Medical Science, Kyoto, Japan, [5]Department of Paediatrics, Ibaraki Children's Hospital, Mito, Japan, [6]Division of Cell Regeneration and Transplantation, Nihon University Graduate School of Medicine, Tokyo, Japan, [7]Department of Transfusion, Toho University School of Medicine, Tokyo, Japan, [8]Department of Paediatrics, Toho University School of Medicine, Tokyo, Japan, [9]Division of Haematology/Oncology, Children's Medical Centre, Japanese Red Cross Nagoya First Hospital, Nagoya, Japan, [10]Department of Haematology, Kanagawa Children's Medical Centre, Yokohama, Japan, [11]Department of Paediatrics, Kyoto University Graduate School of Medicine, Kyoto, Japan, [12]Department of Paediatrics, Kyushu University Graduate School of Medicine, Fukuoka, Japan, and [13]Department of Paediatrics, Nagoya University Graduate School of Medicine, Nagoya, Japan

Received 10 July 2006; accepted for publication 4 September 2006

Correspondence: Ryoji Kobayashi Department of Paediatrics, Hokkaido University Graduate School of Medicine North 15-West 7, Kitaku Sapporo 060-8638, Japan.
E-mail: r-koba@med.hokudai.ac.jp

Summary

The incidence of graft rejection was determined in 66 children with acquired aplastic anaemia (AA) following bone marrow transplantation (BMT) from a related donor. Eleven of 65 evaluable patients experienced either early or late rejection. Multivariate analysis identified previous immunosuppressive therapy with antithymocyte-globulin (ATG) and ciclosporin (CsA) as a risk factor for graft rejection (relative risk: 16·6, $P = 0{\cdot}001$). Patients who received ATG and CsA had a significantly lower probability of failure-free survival than those who did not (69·7 ± 6·2% vs. 87·9 ± 8·0%, $P = 0{\cdot}044$). These results suggest that BMT should be instituted immediately in children with severe AA who have human leucocyte antigen-identical siblings.

Key words: bone marrow transplantation, immunosuppressive therapy, aplastic anaemia, childhood.

  doi:10.1111/j.1365-2141.2006.06352.x

Immunosuppressive therapy (IST) is less expensive and has a lower associated incidence of treatment-related mortality and morbidity. Thus, several researchers have proposed evaluating IST as an initial therapy even in patients with severe aplastic anaemia (AA) who have sibling donors. This therapy would be followed by bone marrow transplantation (BMT) only in patients with inadequate response to IST or relapse (Lawlor *et al*, 1997; Fuhrer *et al*, 2005).

Since 1992, we have conducted a prospective multi-centre study of childhood AA (Kojima *et al*, 2000). In our study, BMT was used for patients with severe or very severe AA who had a human leucocyte antigen (HLA)-identical sibling. Combined IST with antithymocyte-globulin (ATG) and ciclosporin (CsA) was indicated for patients with non-severe AA, even if they had an HLA-identical sibling. However, 33 of 340 patients with severe or very severe AA received IST followed by BMT based on their family's choice, even if they had an HLA-identical sibling. This led us to examine the effect of preceding IST in AA patients who underwent BMT from an HLA-identical sibling to determine whether preceding IST has a detrimental effect on such patients.

Patients and methods

Sixty-six patients with acquired AA who underwent allogeneic BMT from an HLA-identical sibling between November 1992 and September 2004 were enrolled in the study. The diagnosis and assessment of disease severity were established according to published criteria (Camitta *et al*, 1979). The patients were aged between 0 and 18 years (median: 9 years), and 54 had received some form of specific treatment for AA before transplantation, including the following: ATG, CsA, and granulocyte colony-stimulating factor (G-CSF; $n = 21$); ATG and CsA ($n = 12$); G-CSF alone ($n = 10$); CsA with or without steroids ($n = 6$); and CsA with or without steroids and G-CSF ($n = 5$). The following conditioning regimens were used: cyclophosphamide (200 mg/kg) and ATG (Thymoglobulin, Sangstat, Lyon, France: 10 mg/kg) in 39 patients; fludarabine (120 mg/kg), cyclophosphamide (3000 mg/m^2) and 3 Gy of total-lymphoid-irradiation (TLI) or thoraco-abdominal-irradiation in 14 patients; cyclophosphamide (200 mg/kg) and TLI or total-body-irradiation in eight patients; and other regimens in five patients. Graft-*versus*-host-disease (GVHD) prophylaxis, consisting of a combination of methotrexate (MTX) and CsA, was used in 54 patients. The remaining patients received GVHD prophylaxis consisting of CsA, CsA plus steroids, or tacrolimus plus MTX.

Definitions

Failure-free survival (FFS) was defined as survival with sustained engraftment; death and graft-rejection were categorised as treatment failures. Studies on donor chimaerism were performed at each participating hospital by fluorescence *in situ* hybridisation of Y chromosomes or by study of the genetic polymorphism of variable numbers of tandem repeat short DNA sequences of marrow or peripheral blood cells. We assessed complete or mixed donor chimaerism according to previously described criteria (Hoelle *et al*, 2004). Treatment response following BMT is same as response after IST and has been described previously (Kojima *et al*, 2000).

Statistical analysis

Analyses of overall survival and FFS were performed using the Kaplan–Meier method, with differences compared by log-rank and Wilcoxon test. In univariate analysis, the χ^2-test and Fisher's exact test were used to assess risk factors for graft-rejection. P-values $< 0{\cdot}05$ were considered significant. Multivariate stepwise regression was performed to explore the independent effects of variables that showed a significant influence in univariate analysis.

Results

One patient died of septicaemia before the evaluation of engraftment. Of the 65 evaluable patients, two (3%) failed to engraft, and late graft-rejection occurred in nine (14%) of the 63 engrafted patients. The median time to late graft-rejection was 130 days after BMT (40–413 days). Thus, 11patients (17%) experienced early or late graft-rejection: among these patients, one showed recovery of autologous marrow function; two of four patients achieved partial recovery of bone marrow function following donor lymphocyte infusion; and five underwent successful second bone marrow grafts. Of the nine patients in whom donor chimaerism was studied, eight were mixed chimeras at the time of graft-rejection (15–90% donor type), and the remaining patient was a complete chimera with 100% donor-type haematopoietic cells.

In the univariate analysis, two variables were associated with graft-rejection: (1) history of IST with ATG–CsA and (2) the method of GVHD prophylaxis. Patients who received preceding therapy with ATG–CsA had a significantly higher incidence of graft-rejection compared with those who did not receive this therapy ($P = 0{\cdot}044$). Similarly, patients who received GVHD prophylaxis other than CsA and MTX had a significantly higher incidence of graft-rejection ($P = 0{\cdot}022$). In the multivariate analysis, the same variables remained statistically significant; the relative risk of graft-rejection was much higher in patients who received ATG–CsA than in those who did not (relative risk, 16·6; 95% confidence interval, 1·87–146·7; $P = 0{\cdot}001$).

There were considerably more cases of rejection and mixed chimaerism in patients that received previous ATG–CsA, compared with those that did not receive prior ATG–CsA (Table 1, $P < 0{\cdot}05$). The survival rate did not differ between patients who received ATG–CsA and those who did not (97·0% vs. 93·9%, respectively), but the probability of FFS at 8 years was 86·8 ± 6·2% in ATG–CsA recipients compared

Table 1. Comparison of characteristics of children with aplastic anaemia who underwent transplantation with and without prior ATG and CsA.

	ATG and CsA ($n = 33$)	No ATG and CsA ($n = 33$)	P-value
Gender (M/F)	16/17	15/18	NS
Age (years)	10 (0–15)	7 (0–18)	NS
Severity at transplantation: VS	8	14	NS
S	17	16	
Non-S	8	3	
Aetiology: idiopathic	32	32	NS
Hepatitis	1	1	
Diagnosis to transplantation (months)	9·6 (1–59)	2 (0–136)	NS
Transfusion: RC	8 (0–72)	6 (0–44)	<0·05
PC	10·5 (2–55)	8 (0–70)	NS
Conditioning			<0·05
CY + ATG/ALG	15	20	
Flu + CY + TLI/TAI	5	10	
Flu + CY + ATG/ALG	1	2	
CY + TLI	5	0	
Other	7	1	
GVHD prophylaxis			NS
MTX + CsA	27	30	
MTX + FK506	4	0	
CsA + mPSL	1	0	
CsA	1	3	
Infused cell counts ($\times 10^8$/kg)	4·0	3·7	NS
AGVHD (≥grade II)	2	1	NS
CGVHD	3	2	NS
Graft	30	33	NS
Survival	32	31	NS
Late rejection	7	2	NS
Mixed chimerism	12	4	<0·05
Re-transplantation	4	1	NS
Treatment effect (includes re-transplantation)			NS
CR	23	25	
PR	6	5	

VS, very severe; S, severe; Non-S, not severe; CY, cyclophosphamide; ATG, antithymocyte globulin; ALD, antilymphocyte globulin; Flu, fludarabine; TLI, total lymphoid irradiation: TAI, total abdominal irradiation; GVHD, graft-*versus*-host disease; aGVHD, acute GVHD; cGVHD, chronic GVHD; MTX, methotrexate; CsA, ciclosporin; FK506, tacrolimus; mPSL, methylprednisolone; CR, complete response; PR, partial response; NS, not significant; RC, red cell; PC, platelet concentration.

with 69·7 ± 8·0% for those that did not receive ATG–CsA ($P = 0·044$, Fig 1).

Discussion

Ades *et al* (2004) recently analysed risk factors for survival in 133 patients with severe AA who received BMT from HLA-identical siblings. In their study, the 10-year survival estimate was 64%. Due to progress in transplantation and supportive care over the last 2 decades, the survival rate has dramatically improved, from <60% to >90%. Multivariate analysis in the study by Ades *et al* (2004) showed that use of any form of specific treatment prior to BMT had a detrimental effect on overall survival rate. The kinds of specific treatments included androgen ($n = 39$), ATG ($n = 32$), and CsA ($n = 17$), which is of concern as the use of combined ATG–CsA therapy is currently a standard regimen in IST. In our study, use of a specific treatment for AA was not associated with an increased incidence of graft-rejection ($P = 0·673$), but the use of combined IST with ATG and CsA was a significant risk factor for graft-rejection ($P = 0·044$). The incidence of graft-rejection was the same between patients who did or did not receive G-CSF. In conclusion, our data suggest that the overall survival rate is excellent in patients with AA who receive BMT from HLA-identical siblings, but FFS is still unsatisfactory because of a high incidence of graft-rejection. Based on our results and the report from the Saint Louis Hospital (Ades *et al*, 2004), BMT should be instituted

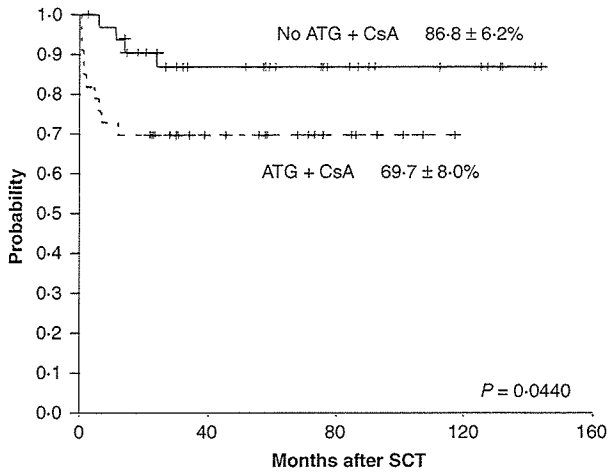

Fig 1. Kaplan–Meier estimate of failure-free survival for patients who did (ATG–CsA) and did not (no ATG–CsA) receive prior immunosuppressive therapy with ATG and CsA: ATG–CsA ($n = 33$): 69·7 ± 8·0%, no ATG-CsA ($n = 33$): 86·8 ± 6·2%, $P = 0·0440$. Failure-free survival was defined as survival with sustained engraftment, whereas death, graft-rejection and late graft-rejection were categorised as treatment failures.

immediately without IST in children with severe SAA who have an HLA-identical sibling.

Acknowledgements

Explanation of authors' contributions: R. Kobayashi analysed data and wrote the paper, H. Yabe, J. Hara, A. Morimoto, M. Tsuchida, H. Mugishima, A. Ohara, I. Tsukimoto, K. Kato, H. Kigasawa, K. Tabuchi, T. Nakahata and S. Ohga designed the research, S. Kojima designed the research, analysed data and wrote the paper.

Research grants and other financial support: None.

References

Ades, L, Mary, JY, Robin, M, Ferry, C, Porcher, R, Esperou, H, Ribaud, P, Devergie, A, Traineau, R, Gluckman, E, Socie, G. (2004) Long-term outcome after bone marrow transplantation for severe aplastic anemia. *Blood*, **103**, 2490–2497.

Camitta, BM, Thomas, ED, Nathan, DG, Gale, RP, Kopecky, KJ, Rappeport, JM, Santos, G, Gordon-Smith, EC, Storb, R. (1979) A prospective study of androgens and bone marrow transplantation for treatment of severe aplastic anemia. *Blood*, **53**, 504–514.

Fuhrer, M, Rampf, U, Baumann, I, Faldum, A, Niemeyer, C, Janka-Schaub, G, Friedrich, W, Ebell, W, Borkhardt, A, Bender-Goetze, C. (2005) Immunosuppressive therapy for aplastic anemia in children: a more severe disease predicts better survival. *Blood*, **106**, 2102–2104.

Hoelle, W, Beck, JF, Dueckers, G, Kreyenberg, H, Lang, P, Gruhn, B, Fuhrer, M, Niethammer, D, Klingebiel, T, Bader, P. (2004) Clinical relevance of serial quantitative analysis of hematopoietic chimerism after allogeneic stem cell transplantation in children for severe aplastic anemia. *Bone Marrow Transplantation*, **33**, 219–223.

Kojima, S, Hibi, S, Kosaka, Y, Yamamoto, M, Tsuchida, M, Mugishima, H, Sugita, K, Yabe, H, Ohara, A, Tsukimoto, I. (2000) Immunosuppressive therapy using antithymocyte globulin, cyclosporin, and danazol with or without human granulocyte colony-stimulating factor in children with acquired aplastic anemia. *Blood*, **96**, 2049–2054.

Lawlor, ER, Anderson, RA, Davis, JH, Fryer, CJ, Pritchard, SL, Rogers, PC, Wu, JK, Schultz, KR. (1997) Immunosuppressive therapy: a potential alternative to bone marrow transplantation as initial therapy for acquired severe aplastic anemia in childhood? *Journal of Pediatric Hematology and Oncology*, **19**, 115–123.

STEM CELLS
EMBRYONIC STEM CELLS

Identification and Characterization of Hemoangiogenic Progenitors During Cynomolgus Monkey Embryonic Stem Cell Differentiation

KATSUTSUGU UMEDA,[a] TOSHIO HEIKE,[a] MOMOKO YOSHIMOTO,[a] GEN SHINODA,[a] MITSUTAKA SHIOTA,[a] HIROFUMI SUEMORI,[b] HONG YUAN LUO,[c] DAVID H. K. CHUI,[c] RYUZO TORII,[d] MASABUMI SHIBUYA,[e] NORIO NAKATSUJI,[f] TATSUTOSHI NAKAHATA[a]

[a]Department of Pediatrics, Graduate School of Medicine, [b]Laboratory of Embryonic Stem Cell Research, Stem Cell Research Center, Institute for Frontier Medical Sciences, [f]Department of Development and Differentiation, Institute for Frontier Medical Science, Kyoto University, Kyoto, Japan; [c]Department of Medicine, Boston University School of Medicine, Boston, Massachusetts, USA; [d]Research Center for Animal Life Science, Shiga University of Medical Science, Ohtsu, Japan; [e]Division of Genetics, Institute of Medical Science, University of Tokyo, Tokyo, Japan

Key Words. Embryonic stem cell • Primate • Hemangioblast • Vascular endothelial growth factor

ABSTRACT

We identified intermediate-stage progenitor cells that have the potential to differentiate into hematopoietic and endothelial lineages from nonhuman primate embryonic stem (ES) cells. Sequential fluorescence-activated cell sorting and immunostaining analyses showed that when ES cells were cultured in an OP9 coculture system, both lineages developed after the emergence of two hemoangiogenic progenitor-bearing cell fractions, namely, vascular endothelial growth factor receptor (VEGFR)-2^{high} CD34^{-} and VEGFR-2^{high} CD34^{+} cells. Exogenous vascular endothelial growth factor increased the proportion of VEGFR-2^{high} cells, particularly that of VEGFR-2^{high} CD34^{+} cells, in a dose-dependent manner. Although either population of VEGFR-2^{high} cells could differentiate into primitive and definitive hematopoietic cells (HCs), as well as endothelial cells (ECs), the VEGFR-2^{high} CD34^{+} cells had greater hemoangiogenic potential. Both lineages developed from VEGFR-2^{high} CD34^{-} or VEGFR-2^{high} CD34^{+} precursor at the single-cell level, which strongly supports the existence of hemangioblasts in these cell fractions. Thus, this culture system allows differentiation into the HC and EC lineages to be defined by surface markers. These observations should facilitate further studies both on early developmental processes and on regeneration therapies in human. STEM CELLS *2006;24:1348–1358*

INTRODUCTION

It has been reported previously that development of hematopoietic cells (HCs) and endothelial cells (ECs) is closely associated [1, 2]. These observations suggest that both lineage cells share a common precursor, which has been called the hemangioblast. Further supporting the putative existence of the hemangioblast is an immunohistochemical study of murine embryos that revealed HC clusters adhering to the ventral floor of the dorsal aorta [3]. Additionally, both HCs and ECs share common surface markers such as vascular endothelial growth factor receptor (VEGFR)-2, CD34, CD31, tyrosine kinase with Ig and EGF homology domain (Tie)-1, and Tie-2 [3, 4]. Of these antigens, VEGFR-2 (also known as Flk-1 in the mouse) is a candidate marker for hemangioblasts, given that murine embryos or ES cells that do not express VEGFR-2 completely fail to produce cells from either lineage [5, 6]. Moreover, recent studies on the differentiation of murine ES cells have shown that both HCs and ECs can be generated from VEGFR-2^{+} cells under various culture conditions [7, 8].

Some immunohistochemical studies of human embryos have shown a spatially close association in the development of both HCs and ECs [9–11]. However, the developmental relationship between HCs and ECs in human embryogenesis has not been further elucidated because of various obstacles, including the ethical restrictions on experiments using human embryos.

To understand the mechanisms that regulate the differentiation of HCs and ECs in humans, it is currently promising to use primate (human and monkey) ES cells. We have recently

Correspondence: Tatsutoshi Nakahata, M.D., Ph.D., Department of Pediatrics, Graduate School of Medicine, Kyoto University, 54 Kawahara-cho, Shogoin, Sakyo-ku, Kyoto 606-8507, Japan. Telephone: 81-75-751-3290; Fax: 81-75-752-2361; e-mail: tnakaha@kuhp.kyoto-u.ac.jp Received April 11, 2005; accepted for publication December 15, 2005; first published online in STEM CELLS *EXPRESS* January 12, 2006. 1066-5099/2006/$20.00/0 doi: 10.1634/stemcells.2005-0165

established a culture system, which induces hematopoietic cell differentiation from cynomolgus monkey ES cells by coculture with OP9 stromal cells [12]. We investigated the close association of HC and EC development during ES cell differentiation in this culture system using fluorescence-activated cell sorting (FACS) and subsequent culture of the sorted fractions. Here, we show that both lineages developed after VEGFR-2^{high} cells emerged on day 6, when neither lineage was observed. Both HCs and ECs were generated from single-cell cultures of VEGFR-2^{high} cells, which strongly supports the existence of hemangioblasts in primates.

Materials and Methods

Cell Lines

The ES cell line CMK6, which was established from cynomolgus monkey blastocysts, was maintained as described previously [13]. The enhanced green fluorescent protein (GFP)-transfected ES cell subline, which we established previously [14], was used to distinguish ES cell-derived cells, except in the experiments that involved immunostaining with antibodies (Abs) to human hemoglobin. The OP9 stromal cell line, a kind gift from Dr. Hiroaki Kodama, was maintained as previously reported [12].

Cytokines and Growth Factors

Recombinant human granulocyte colony-stimulating factor (G-CSF), erythropoietin (EPO), interleukin (IL)-3, and stem cell factor (SCF) were kindly provided by Kirin Brewery (Tokyo, http://www.kirin.co.jp/english). Recombinant human vascular endothelial growth factor (VEGF) was purchased from R&D Systems (Minneapolis, http://www.rndsystems.com).

Antibodies

The primary Abs used in this study were mouse anti-human CD34 (clone 563) and CD41a (clone HIP8) (BD Pharmingen, San Diego, http://www.bdbiosciences.com/pharmingen); mouse anti-human c-kit and rabbit anti-human vWF (Nichirei, Tokyo, http://www.nichirei.co.jp), mouse anti-human CD45 (clone 2B11+PD7/26), and CD41 (clone 5B12) (DAKO, Kyoto, Japan, http://www.dako. com), mouse anti-human vascular endothelial cadherin (VE-cadherin, clone TEA1/31) (Immunotech, Luminy, France, http://www.immunotech.com), mouse anti-human CD31 (clone WM59) (eBioscience, San Diego, CA, http://baybio.co.jp), mouse anti-human CD11b (clone Bear1) (Beckman Coulter, Fullerton, CA, http://www.beckmancoulter.com), rabbit anti-human hemoglobin (Hb) (Cappel, Aurora, OH), mouse anti-human γ-globin (Hbγ) (Santa Cruz Biotechnology, Santa Cruz, CA, http://www.scbt.com), and mouse anti-TRA-1–60 (clone TRA-1–60) (Chemicon, Temecula, CA, http://www.chemicon.com). Mouse anti-stage-specific embryonic antigen (SSEA)-4 monoclonal antibody (mAb) developed by Kannagi et al. [15] was obtained from the Developmental Studies Hybridoma Bank developed under the auspices of the National Institute of Child Health and Human Development and maintained by the Department of Biological Sciences, University of Iowa (Iowa City, IA). The mouse anti-human ε-globin (Hbε) [16] and VEGFR-2 mAbs [17] were used as previously reported. All primary antibodies against human antigens that were used in this study cross- react to cynomolgus monkey proteins, as previously reported [12, 18, 19]. The secondary Abs used in this study were Cy3-conjugated donkey anti-mouse IgG, horseradish peroxidase-conjugated donkey anti-mouse IgG, fluorescein isothiocyanate (FITC)-conjugated donkey anti-rabbit IgG, and alkaline phosphatase (ALP)-conjugated donkey anti-mouse IgG (Jackson ImmunoResearch Laboratories Inc, West Grove, PA, http://www.jacksonimmuno.com), phycoerythrin (PE)-conjugated goat anti-mouse IgG (Dako), PE-conjugated goat anti-mouse IgM (eBioscience), and allophycocyanin (APC)-conjugated goat anti-mouse IgG (BD Pharmingen).

Staining and the Dil-Ac-LDL Incorporation Assay

May-Giemsa staining and immunostaining were performed as previously reported [12]. For the 1,1′-dioctadecyl-1,3,3,3′,3′-tetramethylindocarbocyanine-labeled acetylated low-density lipoprotein (Dil-Ac-LDL) incorporation assay, adherent cells were incubated with 10 μg/ml Dil-Ac-LDL (Molecular Probes Inc., Eugene, OR, http://probes.invitrogen.com) in culture medium for 4 hours at 37°C. These cells were then washed with α-minimum essential medium (α-MEM) (Gibco, Grand Island, NY, http://www.invitrogen.com) and observed by fluorescence microscopy (FLUOVIEW System; Olympus, Tokyo, http://www.olympus-global.com). After the DiI-Ac-LDL incorporation assay, the cells were then fixed and used for antibody staining.

FACS Analysis and Cell Sorting

Staining procedures, FACS analysis, and cell sorting were performed as reported previously [12]. Briefly, the cultured cells were harvested with cell dissociation buffer (Invitrogen, Carlsbad, CA, http://www.invitrogen.com) and incubated with PE- or APC-conjugated Abs or unconjugated Abs for 30 minutes. Samples stained with unconjugated Abs were then incubated with PE- or APC-conjugated goat anti-mouse Abs. Nonviable cells were excluded from the analysis by propidium iodide costaining. FACS analysis was performed with a FACScaliber instrument with the CellQuest program (Becton Dickinson Labware, Bedford, MA, http://www.bd.com). Cell sorting with PE-conjugated CD34 and APC-conjugated VEGFR-2 mAbs was performed using a FACSVantage flow cytometer (Becton Dickinson).

Reverse Transcription-Polymerase Chain Reaction

RNA isolation and reverse transcription-polymerase chain reaction (RT-PCR) were performed as described previously [12]. Samples were initially denatured at 94°C for 5 minutes, followed by 35–40 amplification rounds consisting of 94°C for 1 minute (denaturing), 60°C for 1 minute (annealing), and 72°C for 1 minute (extension), followed by a final extension at 94°C for 7 minutes. The primers used for RT-PCR were as follows: GATA-1 (498 bp), forward, 5′-CAC ATC CCC AAG GCG GCC GAA C-3′, reverse, 5′-AGG TCT GGG CTC AGC CGC TCT-3′; MYB (307 bp), forward, 5′-CAC GCT GGG CCT GTC ATC AAC-3′, reverse, 5-GCA TGG CTC TTC GTG TTA TAG C-3′; FLI-1 (412 bp), forward, 5′-ATG GAT CCA GGG AGT CTC CGG T-3′, reverse, 5′-TTG GTC GGT GTG GGA GGT TGT-3′; Tie-1 (308 bp), forward, 5′-TGG TCG GAG AGA ACC TAG CC-3′, reverse, 5′-GAC GCA TCA GCT CGT ACA CTT C-3′; eNOS (557 bp), forward, 5′-GAC ATT TTC GGG CTC ACG CTG-3′, reverse, 5′-TGG GGT AGG CAC TTT AGT AGT TC-3′; GATA-2 (303 bp), forward, 5′-TGG CGC ACA ACT ACA TGG AAC-3′, reverse, 5′-GAG GGG TGC AGT GGC GTC TT-3′; SCL (185 bp), forward, 5′-TCT

CGG CAG CGG GTT CTT TG-3′, reverse, 5′-AAG GCC CCG TTC ACA TTC TGC-3′; FLT-1 (508 bp), forward, 5′-GCT CAC CAT GGT CAG CTA CTG-3′, reverse, 5′-CAG TGA TGT TAG GTG ACG TGA ACC-3′; Rex-1 (489 bp), forward, 5′-CGC GGT GTG GGC CTT ATG TG-3′, reverse, 5′-TCT CAG GGC AGC TCT ATT CCT C-3′; Oct-4 (246 bp), forward, 5′-CGT GAA GCT GGA GAA GGA GAA GCT G-3′, reverse, 5′-CAA GGG CCG CAG CTT ACA CAT GTT C-3′; GAPDH (360 bp), forward, 5′-CAC CAG GGC TGC TTT TAA CTC TG-3′, reverse, 5′-ATG GTT CAC ACC CAT GAC GAA C-3′. cDNA from cynomolgus monkey bone marrow, human umbilical vein endothelial cells (HUVECs), and human erythroleukemia K562 cells served as positive controls. For semiquantitative comparisons, samples were normalized by dilution to give equivalent signals for GAPDH.

In Vitro Differentiation of ES Cells

For initial differentiation induction, trypsin-treated undifferentiated ES cells were transferred onto fresh confluent OP9 cells in six-well plates at a concentration of 4×10^3 cells per well and cultured with various concentrations of VEGF (0, 10, 20, and 40 ng/ml) in α-minimum essential medium supplemented with 10% fetal calf serum (FCS) (Sigma-Aldrich, St. Louis, http://www.sigmaaldrich.com) and 50 μM 2-mercaptoethanol (2ME). The cultured cells were harvested in cell dissociation buffer (Invitrogen) and analyzed by FACS, as described above, on days 4, 6, 8, and 10.

To induce the differentiation of HCs and ECs, cells that had been cultured for 6 days in the presence of 20 ng/ml VEGF were harvested and sorted by FACS according to the expression of VEGFR-2 and CD34, as detailed in Results. Each sorted cell fraction was transferred onto fresh confluent OP9 cells in six-well plates at a concentration of 1×10^4 cells per well or in 12-well plates at a concentration of 1×10^3 cells per well. To analyze the development of HCs, the sorted cells were cultured in α-MEM supplemented with 10% FCS (Sigma-Aldrich), 50 μM 2ME, and a mixture of 10 ng/ml G-CSF, 2 U/ml EPO, 20 ng/ml IL-3, and 100 ng/ml SCF (hematopoietic cytokine mixture). Floating and adherent HCs were analyzed sequentially, as previously reported [12, 20]. To analyze EC development, the sorted cells were cultured in α-MEM supplemented with 10% FCS, 50 μM 2ME, and 20 ng/ml VEGF. Six days after cell sorting, the cells were stained with anti-VE-cadherin and ALP-conjugated anti-mouse IgG, and the EC clusters were scored by microscopy. At least three independent experiments were conducted.

Single-Cell Deposition Assay for Hematopoietic and Endothelial Differentiation

The deposition of single sorted cells into individual wells of 96-well plates was carried out by using the Clon-Cyt system of the FACSVantage flow cytometer (Becton Dickinson). Individual sorted cells from each fraction were seeded onto OP9 stromal cells in α-MEM supplemented with 10% FCS and a hematopoietic cytokine mixture. After 6 days in culture, HC development was evaluated by immunostaining with the anti-CD45, CD41, and HbF mAbs, whereas EC development was analyzed by immunostaining with the anti-VE-cadherin mAb or by the DiI-Ac-LDL incorporation assay. The concomitant development of both lineage of cells was confirmed by immunostaining with the anti-CD34 mAb.

Statistics

Differences in the number of HC or EC cluster between two groups were assessed using Student's t test. Differences in the frequency of HC and/or EC cluster development in the single-cell deposition assay were assessed using the χ^2 test. Statistical significance was defined as p values less than .05.

RESULTS

FACS Analysis of Hematopoietic and/or Endothelial Surface Markers During Early Primate ES Differentiation

The ES cell line CMK6 and the GFP-transfected ES cell subline that were used in this study both expressed the undifferentiated-state marker SSEA-4, even after being maintained in culture for more than a year (data not shown). We confirmed that both ES cell lines were equally capable of differentiating into HCs and ECs (data not shown).

By RT-PCR analysis of cultures in the OP9 coculture system, we have demonstrated previously that sequential expression of genes associated with both HC and EC lineage development was equivalent to that seen during primate ontogeny in vivo [12]. FACS analysis was used to determine the expression patterns of various surface markers involved in HC and EC development when GFP-transfected ES cells were induced to differentiate by coculture with OP9 stromal cells in the presence or absence of exogenous VEGF (Fig. 1). The numbers of cells expressing particular markers were quantified as a percent of the total live GFP^+ cells in the culture (Fig. 1A). Although substantial fraction of the GFP^+ cells were dead after being harvested with cell dissociation buffer, harvesting by other means, such as by using trypsin or collagenase, did not significantly alter the proportion of dead cells (data not shown). The markers could be classified into three groups depending on their expression kinetics. The first group includes CD34 and CD31, which are expressed by both early HCs and ECs (Fig. 1B, 1C). Their expression was not detected in undifferentiated ES cells, but became upregulated on day 6. Thereafter, $CD34^+$ and $CD31^+$ cells increased, especially in the presence of exogenous VEGF. The second group includes CD45, CD41a, and VE-cadherin (Fig. 1D–1F), whose expression is specific to either HCs (CD45 and CD41a) or ECs (VE-cadherin). Expression of these proteins was not detected in undifferentiated ES cells but became slightly upregulated by day 10 in the presence of VEGF. The third group includes c-kit and VEGFR-2 (Fig. 1G, 1H). Although expression of these proteins was detected in almost all undifferentiated ES cells, it became downregulated on day 4 and thereafter, with or without exogenous VEGF. These kinetics were similar to that of SSEA-4 (Fig. 1I), which is expressed by undifferentiated ES cells [13, 21]. These observations showed that during in vitro HC and EC differentiation, common surface markers such as CD34 and CD31 were expressed first, followed by the expression of lineage-specific markers.

Generation of VEGFR-$2^{high}CD34^-$ and VEGFR-$2^{high}CD34^+$ Cells Before HC or EC Development During Primate ES Cell Differentiation

Several studies have demonstrated that VEGFR-2 is a key marker of hemangioblasts during early murine development [5–8]. CD34 and CD31 are also expressed by early

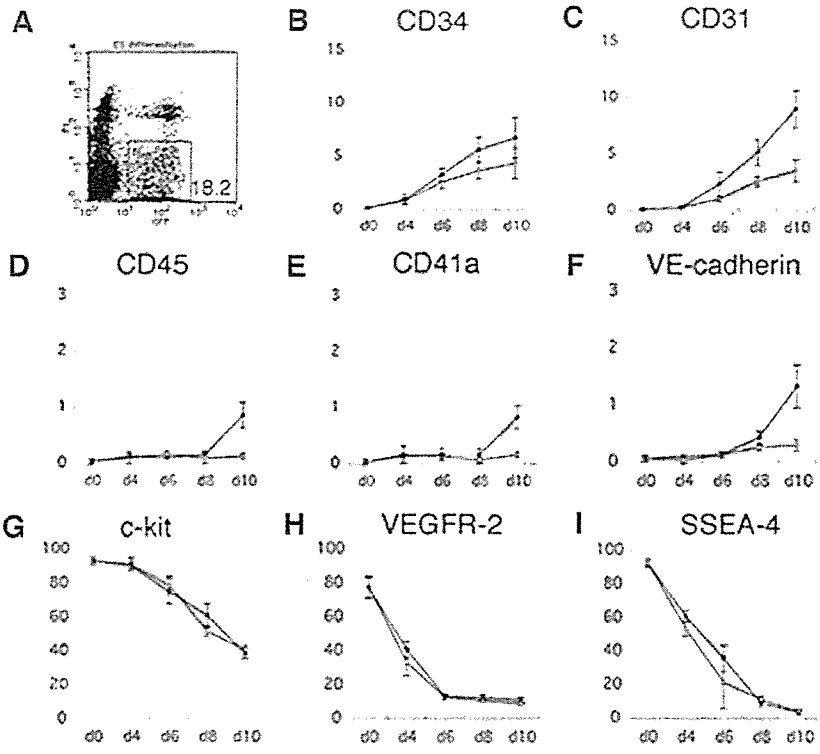

Figure 1. Fluorescence-activated cell sorting (FACS) analysis of surface markers expressed by hematopoietic cells and/or endothelial cells during embryonic stem (ES) cell differentiation. Undifferentiated green fluorescent protein (GFP)-transfected ES cells were seeded onto confluent OP9 stromal cells in six-well plates in the presence or absence of 20 ng/ml exogenous vascular endothelial growth factor (VEGF). The undifferentiated ES cells and the subsequent cultures on days 4, 6, 8, and 10 were stained with various monoclonal antibodies and quantified by FACS analysis. **(A):** The amounts of GFP^+ ES-derived live cells (boxed region) are shown as a percentage of the total cells in cultures. **(B–I):** Cells that stained positive for each antigen, CD34 **(B)**, CD31 **(C)**, CD45 **(D)**, CD41a **(E)**, VE-cadherin **(F)**, c-kit **(G)**, VEGFR-2 **(H)**, and SSEA-4 **(I)**, are shown as a percentage of the total GFP^+ cells. The white and black circles show the results in the absence and presence of VEGF, respectively. The data represent the mean ± SD of three independent experiments. Abbreviations: SSEA, stage-specific embryonic antigen; VE-cadherin, vascular endothelial cadherin; VEGFR, vascular endothelial growth factor receptor.

hematopoietic and endothelial progenitors [9, 11]. Therefore, to identify bipotential progenitor cells in primates, we analyzed the differentiating ES cell-derived cells by FACS using VEGFR-2, CD34, and CD31 mAbs. The undifferentiated ES cells did not express CD34 or CD31, whereas approximately 80% of them expressed VEGFR-2 at low levels (Fig. 2A, 2B). We examined the expression levels of VEGFR-2 more closely and found that the proportion of VEGFR-2^{low} cells gradually decreased during coculture and that VEGFR-2^{high} cells could be detected on day 6. More than half of the VEGFR-2^{high} cells were CD34-negative on day 6, but VEGFR-2^{high} $CD34^+$ cells increased by day 8 and thereafter (Fig. 2A). The same temporal expression pattern of CD31 among the VEGFR-2^{high} cells was observed (Fig. 2B). FACS and immunostaining analysis showed that the VEGFR-2^{high} cells that emerged on day 6 were negative for CD41a, CD45, VE-cadherin, or any hemoglobins (data not shown), indicating that these cells did not yet express HC or EC lineage-specific markers.

We further examined the differentiation state of the VGEFR-2^{high} cells by double staining with mAbs for VEGFR-2 and TRA-1–60, a surface marker indicative of undifferentiated ES cells. The expression of TRA-1–60 was detected in undifferentiated ES cells, as previously reported [13, 21], and was upregulated on day 4. However, although approximately half of the GFP^+ ES cell-derived cells were positive for TRA-1–60 on day 6 and thereafter, the VEGFR-2^{high} cells were always negative for TRA-1–60 at all time points (Fig. 2C).

To verify the potential of day 6 VEGFR-2^{high} $CD34^-$ and VEGFR-2^{high} $CD34^+$ cells to differentiate into the HC and EC lineages, their gene expression profiles were investigated by RT-PCR. The genes analyzed were those representing HC (GATA-1, MYB, and FLI-1) [22], EC (Tie-1 and eNOS) [23, 24], or HC-EC potentials (SCL, FLT-1, and GATA-2) [25–27]. As shown in Figure 2D, GATA-1 and SCL were expressed by VEGFR-2^{high} $CD34^+$ cells but not by VEGFR-2^{high} $CD34^-$ cells, whereas FLI-1 expression was up-regulated in both VEGFR-2^{high} cell populations. In contrast, the expression profiles of the other HC and/or EC markers did not correlate with the development of VEGFR-2^{high} cells.

We also analyzed the expression of Rex-1 and Oct-4, which are marker genes for undifferentiated ES cells [21]. Although their expression was still detected in the total GFP^+ cell populations on day 6, they were not expressed by either VEGFR-2^{high} cell population. These observations together indicate that the day 6 VEGFR-2^{high} cell population differs from other ES cell-derived cells that emerge during the differentiation induction, as they express genes characteristic for the HC and/or EC lineages.

We then analyzed the effect of VEGF on VEGFR-2^{high} cell development by adding various concentrations of VEGF to the culture (Table 1). FACS analysis demonstrated that the presence of VEGF increased both the proportion of VEGFR-2^{high} cells in the culture and the percentage of VEGFR-2^{high} $CD34^+$ cells among the VEGFR-2^{high} cell fraction. This effect was dose-dependent and saturated at 20 ng/ml VEGF. The same trends were observed by analysis with VEGFR-2 and CD31 mAbs.

HC Development from VEGFR-2^{high} Fractions

Given the results described above, we hypothesized that the VEGFR-2^{high} $CD34^-$ or the VEGFR-2^{high} $CD34^+$ cells on day 6 may contain hemoangiogenic progenitors. As shown in Figure 1D–1F, rather few HCs and ECs develop from ES cells over 10

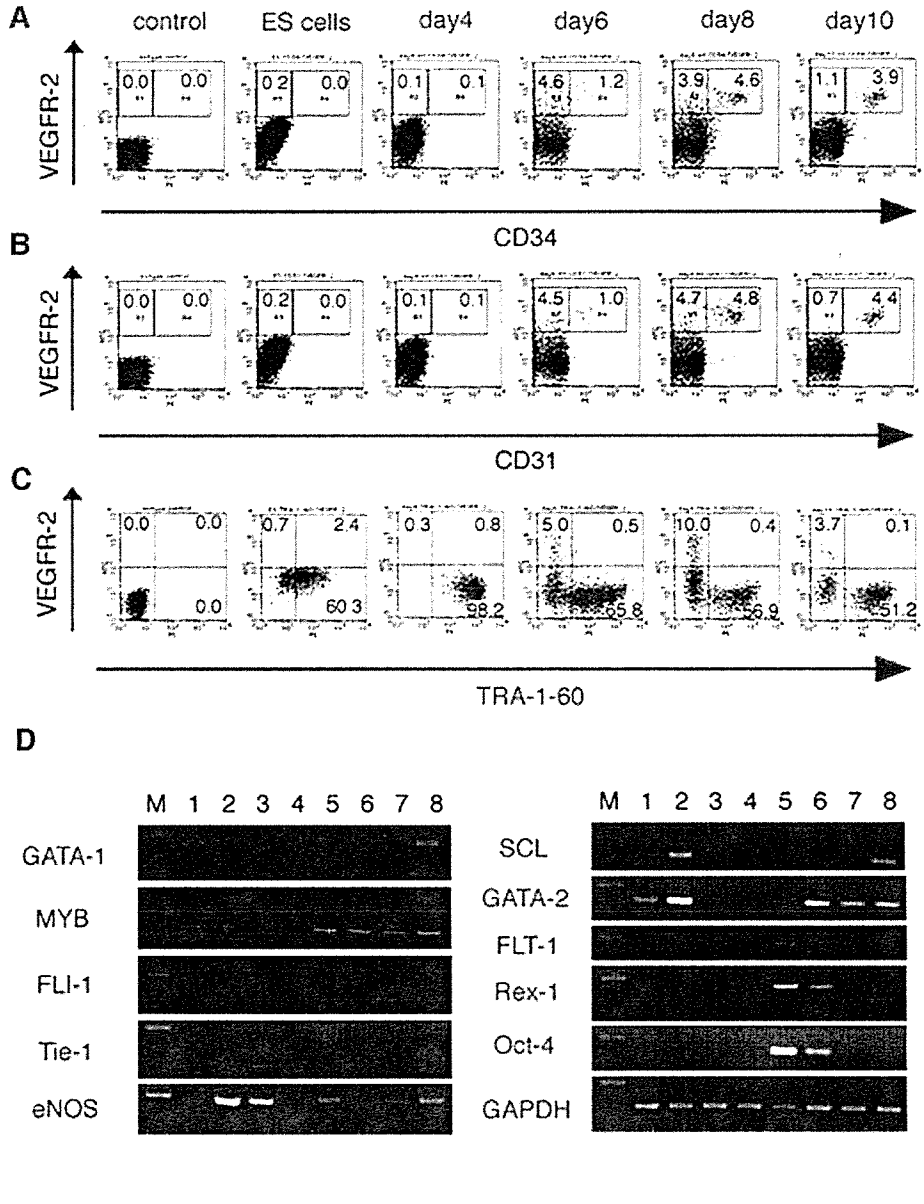

Figure 2. Fluorescence-activated cell sorting and reverse transcription-polymerase chain reaction (RT-PCR) analysis of the VEGFR-2^{high} cells that emerge during ES cell differentiation. The green fluorescent protein (GFP)-transfected ES cells and the subsequent cultures on days 4, 6, 8, and 10 in the absence of exogenous vascular endothelial growth factor were analyzed by FACS with antibodies against VEGFR-2 and CD34 **(A)**, VEGFR-2 and CD31 **(B)**, or VEGFR-2 and TRA-1–60 **(C)**. **(A, B):** The amounts of VEGFR-2^{high} $CD34^-$ or VEGFR-2^{high} $CD31^-$ cells (upper left quadrant), or VEGFR-2^{high} $CD34^+$ or VEGFR-2^{high} $CD31^+$ cells (upper right quadrant), are shown as a percentage of the total GFP^+ ES cells. **(C):** The numbers in each quadrant represent percentages of cells among the total GFP^+ ES cells. **(D):** ES cells cocultured with OP9 cells for 6 days were subjected to RT-PCR analysis of genes associated with HC and/or EC development. The lanes contained mRNA from the following cells: adult cynomolgus monkey bone marrow cells (lane 1), the human erythroblastic cell line K562 (lane 2), human umbilical vein endothelial cells (lane 3), OP9 stromal cells (lane 4), undifferentiated ES cells (lane 5), the total GFP^+ ES cell-derived cells (lane 6), the VEGFR-2^{high} $CD34^-$ cells (lane 7), and the VEGFR-2^{high} $CD34^+$ cells (lane 8), harvested on day 6. Representative results from one of three independent experiments are shown. Abbreviations: EC, endothelial cells; ES, embryonic stem; HC, hematopoietic cells; M, size marker; VEGFR, vascular endothelial growth factor receptor.

Table 1. Effects of VEGF on the generation of VEGFR-2^{high} cells

[VEGF]	VEGFR-2^{high} cells (% of GFP^+ cells)	$CD34^+$ cells (% of VEGFR-2^{high} cells)	$CD31^+$ cells (% of VEGFR-2^{high} cells)
Nil	5.7 ± 0.7	21.2 ± 0.9	18.6 ± 4.4
V10	5.8 ± 0.5	23.8 ± 1.2	23.5 ± 1.2
V20	8.2 ± 0.5	36.0 ± 2.7	30.0 ± 0.6
V40	8.7 ± 1.0	35.0 ± 7.4	35.7 ± 7.5

ES cells were cultured with various concentrations of VEGF (0, 10, 20, and 40 ng/ml; Nil, V10, V20, and V40, respectively) for 6 days, and the resultant cells were then analyzed with monoclonal antibodies specific for VEGFR-2 and CD34, or VEGFR-2 and CD31. The data are displayed as either the average percentage of VEGFR-2^{high} cells among the total live GFP^+ ES cell-derived cells, or the % of the VEGFR-2^{high} $CD34^+$ or $CD31^+$ cells among the total VEGFR-2^{high} cells. All percentages are the mean ± SD of three independent experiments.

Abbreviations: ES, embryonic stem; GFP, green fluorescent protein; VEGF, vascular endothelial growth factor; VEGFR, vascular endothelial growth factor receptor.

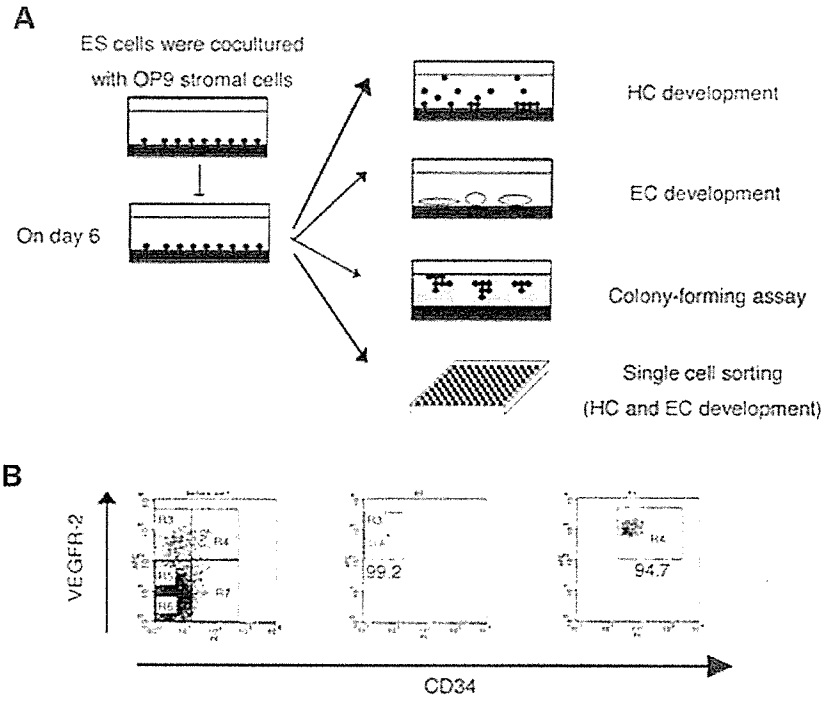

Figure 3. Schematic representation of the assays used to analyze the differentiation of HCs and ECs from ES cells. **(A, B):** The cells were cocultured with OP9 cells in the presence of 20 ng/ml vascular endothelial growth factor (VEGF) and sorted using VEGFR-2 and CD34 mAbs on day 6. The FACS plot **(B)** shows the regions (R3–R7) that were used to define the different populations of cells: VEGFR-2^{high} $CD34^-$, R3; VEGFR-2^{high} $CD34^+$, R4; VEGFR-2^{low} $CD34^-$, R5; VEGFR-2^- $CD34^-$, R6; VEGFR-2^{low} or $-$ $CD34^+$, R7. The sorted cells from each population were then transferred onto fresh confluent OP9 cells. To analyze HC development, the sorted cells were cultured in α-minimum essential medium (α-MEM) supplemented with 10% fetal calf serum (FCS), 2-mercaptoethanol (2ME), and a mixture of granulocyte colony-stimulating factor, erythropoietin, interleukin-3, and stem cell factor (hematopoietic cytokine mixture). The number of adherent HC clusters were counted 4 days after cell sorting, and the floating cells were analyzed every 2 days. To analyze EC development, the sorted cells were cultured in α-minimum essential medium (α-MEM) supplemented with 10% FCS, 2ME, and VEGF. Cultures were analyzed by immunostaining with an antibody against vascular endothelial cadherin 6 days after cell sorting. For the single-cell deposition assay, individual sorted cells from the VEGFR-2^{high} $CD34^-$ and VEGFR-2^{high} $CD34^+$ fractions were seeded onto OP9 stromal cells and cultured with a hematopoietic cytokine mixture. Six days later, HC and EC development was evaluated by immunostaining or by the 1,1′-dioctadecyl-1,3,3,3′,3′-tetramethylindocarbocyanine-labeled acetylated low-density lipoprotein incorporation assay. FACS reanalysis showed that the purity of the sorted VEGFR-2^{high} $CD34^-$ and VEGFR-2^{high} $CD34^+$ cell populations was 99.0%–99.7% and 93.0%–97.0%, respectively (see the right-hand dotplots for examples). Abbreviations: EC, endothelial cell; ES, embryonic stem; HC, hematopoietic cell; VEGFR, vascular endothelial growth factor receptor.

days of culture. However, we have shown previously that the numbers of HCs that develop from ES cells markedly increased if the cells are replated onto a new confluent OP9 cell layer and that abundant hematopoiesis, in particular definitive hematopoiesis, cannot develop without additional VEGF [12]. Therefore, we sorted the cultures using anti-VEGFR-2 and CD34 mAbs after initial 6-day VEGF treatment, and each fraction was replated onto a new confluent OP9 cell layer. Fractions of VEGFR-2^{high} $CD34^-$, VEGFR-2^{high} $CD34^+$, VEGFR-2^{low} $CD34^-$, VEGFR-2^- $CD34^-$, and VEGFR-$2^{low\ or\ -}$ $CD34^+$ cells were collected, replated, and analyzed for their capacity to generate HCs and/or ECs, as shown schematically in Figure 3A. FACS reanalysis of the sorted VEGFR-2^{high} $CD34^+$ cells showed their purity ranged from 93.0%–97.0%, whereas the purity of the other sorted fractions ranged from 99.0%–99.7% (Fig. 3B and data not shown).

Adherent HCs first emerged from the VEGFR-2^{high} $CD34^-$ and VEGFR-2^{high} $CD34^+$ fractions 2 days after cell sorting and replating (Fig. 4A, 4B). The adherent HCs, which formed clusters on or underneath the OP9 stromal layer, are known to contain immature hematopoietic progenitors [12, 20]. Almost all of the adherent HC clusters were positive for CD34 (Fig. 4H) and also contained cells that were positive for VEGFR-2- (Fig. 4I), CD45- (Fig. 4J), CD11b- (Fig. 4K), CD41- (Fig. 4L), and Hbε (Fig. 4M). The number of adherent HC clusters was maximal on day 10 but decreased thereafter. On day 10, the number of clusters generated from the VEGFR-2^{high} $CD34^+$ fraction was approximately four times the number generated from the VEGFR-2^{high} $CD34^-$ fraction. Furthermore, larger clusters were detected from the VEGFR-2^{high} $CD34^+$ fractions (Fig. 4M), and adherent clusters from the VEGFR-2^{high} $CD34^+$ fraction covered the stromal layer by day 20 (Fig. 4E), whereas adherent clusters from the VEGFR-2^{high} $CD34^-$ fraction were rarely observed (Fig. 4D) and disappeared over time in culture.

In this coculture system, HC development in the floating fractions first occurred on day 8 (2 days after seeding on day 6). The floating cells were found to consist exclusively of mature HCs, such as erythrocytes, myeloid lineage cells, and megakaryocytes (data not shown) [12]. We examined whether both VEGFR-2^{high} fractions were capable of both primitive and definitive hematopoiesis by sequential May-Giemsa staining and immunostaining with hemoglobin Abs. Until day 15 (9 days after sorting), all of the floating HCs from both fractions were large nucleated erythrocytes positive for Hbε, Hbγ, and Hb (Fig. 4C, 4N–4Q). These cells correspond to primitive erythrocytes (EryP). On day 18 and thereafter, both VEGFR-2^{high} $CD34^-$ and VEGFR-2^{high} $CD34^+$ cultures contained some small erythrocytes, including enucleated erythrocytes, that were positive for Hbγ and Hb but negative for Hbε (Fig. 4F, 4R–4U). These cells correspond to definitive erythrocytes (EryD). The number of erythrocytes generated from either cell fraction was maximal on day 12 but gradually decreased thereafter. Subsequently, a second wave of erythrocytes appeared around day 21 (Fig. 4W). The proportion of EryD gradually increased around day 18 and